JOURNAL OF GEOPHYSICAL RESEARCH, VOL. 108, NO. D3, 4124, doi:10.1029/2002JD002287, 2003

Daily precipitation statistics in regional climate models: Evaluation and intercomparison for the European Alps

Christoph Frei,[1] Jens Hesselbjerg Christensen,[2] Michel Déqué,[3] Daniela Jacob,[4] Richard G. Jones,[5] and Pier Luigi Vidale[1]

Received 12 March 2002; revised 27 August 2002; accepted 8 September 2002; published 12 February 2003.

[1] An evaluation is undertaken of the statistics of daily precipitation as simulated by five regional climate models using comprehensive observations in the region of the European Alps. Four limited area models and one variable-resolution global model are considered, all with a grid spacing of 50 km. The 15-year integrations were forced from reanalyses and observed sea surface temperature and sea ice (global model from sea surface only). The observational reference is based on 6400 rain gauge records (10–50 stations per grid box). Evaluation statistics encompass mean precipitation, wet-day frequency, precipitation intensity, and quantiles of the frequency distribution. For mean precipitation, the models reproduce the characteristics of the annual cycle and the spatial distribution. The domain mean bias varies between −23% and +3% in winter and between −27% and −5% in summer. Larger errors are found for other statistics. In summer, all models underestimate precipitation intensity (by 16–42%) and there is a too low frequency of heavy events. This bias reflects too dry summer mean conditions in three of the models, while it is partly compensated by too many low-intensity events in the other two models. Similar intermodel differences are found for other European subregions. Interestingly, the model errors are very similar between the two models with the same dynamical core (but different parameterizations) and they differ considerably between the two models with similar parameterizations (but different dynamics). Despite considerable biases, the models reproduce prominent mesoscale features of heavy precipitation, which is a promising result for their use in climate change downscaling over complex topography. *INDEX TERMS:* 3309 Meteorology and Atmospheric Dynamics: Climatology (1620); 3354 Meteorology and Atmospheric Dynamics: Precipitation (1854); 3337 Meteorology and Atmospheric Dynamics: Numerical modeling and data assimilation; 9335 Information Related to Geographic Region: Europe; *KEYWORDS:* climate model evaluation, extreme events, heavy precipitation, climate change downscaling, Alps

Citation: Frei, C., J. H. Christensen, M. Déqué, D. Jacob, R. G. Jones, and P. L. Vidale, Daily precipitation statistics in regional climate models: Evaluation and intercomparison for the European Alps, *J. Geophys. Res.*, *108*(D3), 4124, doi:10.1029/2002JD002287, 2003.

1. Introduction

[2] Regional climate models (RCMs) are promising tools to derive climate change scenarios on spatial scales that are currently not amenable by general circulation models (GCMs) [e.g., *Giorgi et al.*, 2001; *McGregor*, 1997]. RCMs can provide input data for climate impact studies [e.g., *Kite*, 1997; *Mearns et al.*, 1997; *Stone et al.*, 2001] and they serve as experimental tools for the study of regional climate processes [e.g., *Pielke et al.*, 1999; *Pan et al.*, 1999; *Schär et al.*, 1999; *Heck et al.*, 2001]. Moreover, the improved representation of severe weather phenomena, as compared to GCMs, has stimulated numerous RCM applications concerned with the variability, change and impact of extreme events, especially those of heavy precipitation and drought [e.g., *Christensen et al.*, 2001a; *Durman et al.*, 2001; *Jones and Reid*, 2001; *Jones et al.*, 1997; *Räisänen and Joelsson*, 2001; *Seneviratne et al.*, 2002]. Such applications demand for accurate model simulations not only of time-mean conditions but also of the day-to-day (and even subdaily) variability [e.g., *Dai et al.*, 1999; C. J. Andersen et al., Hydrological processes in regional climate model simulations of the central United States flood of June–July 1993, submitted to *Journal of Hydrology*, 2002]. In this context, a rigorous model evaluation of the simulated high-frequency variations and the distribution and frequency of extreme events is an important step in assessing the models' credibility for climate downscaling and climate impact applica-

[1]Atmospheric and Climate Science, Eidgenossische Technische Hochschule, Zurich, Switzerland.
[2]Danish Meteorological Institute, Copenhagen, Denmark.
[3]Météo France, Centre National de Recherches Météorologiques, Toulouse, France.
[4]Max Planck Institute for Meteorology, Hamburg, Germany.
[5]Met Office Hadley Centre, Bracknell, United Kingdom.

0148-0227/03/2002JD002287$09.00

tions and it guides efforts for model improvements. The theme of this study is a comprehensive evaluation and intercomparison of 5 regional European climate models with regard to high-frequency (i.e., daily) precipitation statistics.

[3] The evaluation of high-frequency precipitation statistics is confronted with the complication that observations and model data differ in areal representativity: Rain gauge measurements are point observations. They are influenced by site-specific conditions and their high-frequency statistics carries the signal of small-scale variations of the precipitation systems [e.g., *Goodrich et al.*, 1995]. Precipitation from climate models, on the other hand, represents an area-mean value over a model grid box. The extent to which this may be expected to truly represent precipitation over this area is not clear and may depend for example on the degree of numerical diffusion and the effective resolution of the model topography. A reasonable assumption is that the representative area for simulated precipitation is somewhere between one and four grid boxes. Clearly, even if the RCM is skilful at its grid box resolution, statistics of a model grid box record and a single rain gauge record will be different, the latter will have smaller wet-day frequency, higher mean wet-day amounts and longer tails in the frequency distribution [see *Gregory and Mitchell*, 1995; *Mearns et al.*, 1995; *Osborn and Hulme*, 1997].

[4] The evaluation of daily precipitation statistics thus demands a data network, from which area-mean values can be reliably estimated and model-consistent statistics be derived. The data requirement for this upscaling is however considerable: Based on rain gauge data for the UK, *Osborn and Hulme* [1997] find that the bias of domain–mean precipitation variance and wet-day frequency is larger than 10% when fewer than about 15 stations are used in the areal averaging. The limited accessibility to high-resolution daily precipitation observations by the climate modeling community has impeded the evaluation of precipitation statistics. Evaluations were mostly restricted to large areas for which sufficient spatial sampling was available [e.g., *Durman et al.*, 2001; *Frei et al.*, 1998] or the conclusions were subject to considerable uncertainty due to coarse observation sampling [e.g., *Mearns et al.*, 1995; *Murphy*, 1999]. A reliable assessment of RCM performance near the scale of the model resolution had been difficult to obtain so far.

[5] The purpose of this study is to evaluate the statistics of daily precipitation, as simulated in five European RCMs, by comparison to an observational analysis for the region of the European Alps. The analysis was explicitly derived for this evaluation, is compatible in resolution with that of the climate models, and is based on a comprehensive data set of 6400 rain gauge stations. The density of the observation network, with 10–50 stations in each model/analysis grid box, permits an evaluation at the scale of the model resolution. Attention is given to the uncertainty of the statistics emerging from the unknown effective resolution of the climate models. Evaluation statistics embrace several measures of the daily precipitation frequency distribution including the wet-day frequency, precipitation intensity (average precipitation per wet day), and quantiles of the distribution function.

[6] The complex topography and land–sea distribution of the study area are responsible for numerous mesoscale flow features and precipitation processes in response to synoptic-scale disturbances, primarily during the winter half-year, and more in situ forcing of convection in summer [e.g., *Schär et al.*, 1998]. Clearly, the Alps constitutes an ambitious test ground for regional climate models, but it is also in such regions where the need for climate downscaling is most obvious.

[7] The RCM simulations under consideration were conducted in the framework of a joint project (Modeling European Regional Climate-Understanding and Reducing Errors (MERCURE)), using a comparable experimental setup: Four of the models are limited area models (LAMs) and were driven from reanalyses over the 15 years (1979–1993). The "perfect" boundary forcing keeps biases in the driving fields small (compared to forcing from a free GCM) [e.g., *Pan et al.*, 2001] and allows the isolation of RCM downscaling errors by comparison with observations for the same period [e.g., *Christensen et al.*, 1997; *Lüthi et al.*, 1996]. The remaining model is a variable-resolution GCM, which was driven from observed sea surface temperature and sea ice over the same 15-year period. This model is less constrained than the LAMs and errors may also arise from the lack of predictability and the models' random and systematic errors in the synoptic-scale circulation. Over the Alpine region, all the models exhibit a resolution of about 50 km. An evaluation of the same simulations with respect to the mean surface energy fluxes is given by *Hagemann et al.* [2002] and results from GCM forcing by *Machenhauer et al.* [1998].

[8] The outline of the paper is as follows: The observational reference data and evaluation statistics are presented in section 2, and section 3 gives a brief description of the regional climate models. Results of the evaluation are presented sequentially for the annual cycle of domain mean statistics (section 4.1), the spatial distribution (section 4.2) and the precipitation frequency distributions (section 4.3). A comparison of the simulated statistics for other European regions is given in section 4.4. Section 5 summarizes the results and draws some conclusions.

2. Reference Data and Validation Statistics

2.1. Study Area

[9] The study area of this model validation is a 1100 $\times$ 700 km^2 domain (2.25°–17.25°E, 42.25°–48.75°N), encompassing the ridge of the European Alps and a belt of adjacent foreland terrain (Figure 1a). The main mountain ridge is arc shaped, has a typical crest height of 2500 mMSL, and varies in width between 100 and 300 km. The foreland belt comprises several hill ranges with crest heights of around 1000 mMSL and a spatial scale larger than the model resolution of 50 km. Aside the main study area of the Alps, 4 additional European subdomains (Figure 1b) will be considered for the assessment of intermodel differences in section 4.4.

2.2. Observation Reference

[10] The observational reference, against which the model simulations are being evaluated in the Alpine region, constitutes of gridded precipitation analyses for each day of the period 1979–1993. These analyses were constructed by spatial aggregation of rain gauge observations onto a regular latitude–longitude grid of 0.5° resolution (i.e., grid spacing

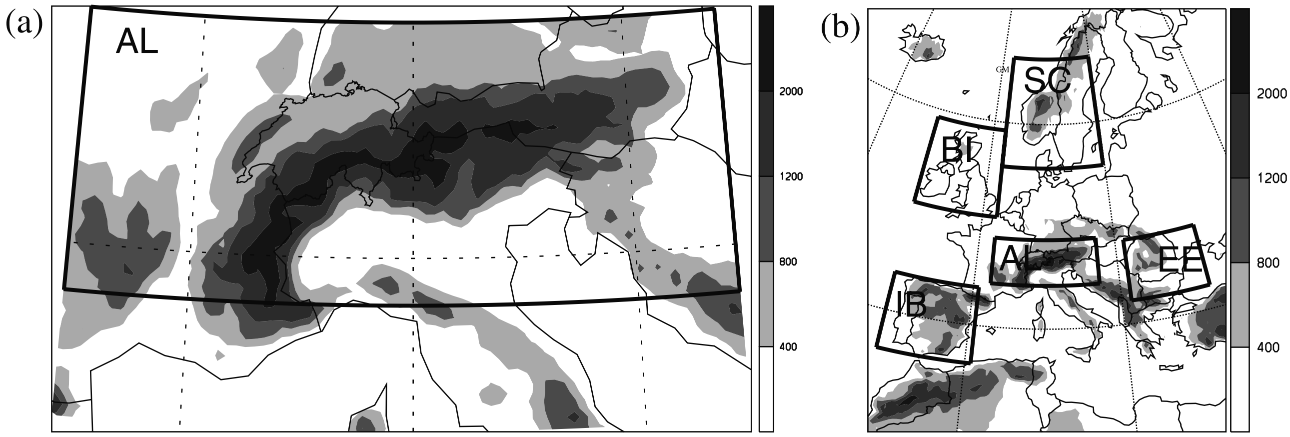

Figure 1. Study areas for model evaluation and intercomparison. Shading represents topographic height in mMSL. (a) Alpine region and (b) additional European regions (AL, Alpine region; BI, British Isles; EE, Eastern Europe; IB, Iberian Peninsula; SC, Scandinavia).

is 56 km N-S, 40 km E-W; grid points are on x.25° and x.75° latitude and longitude).

[11] The underlying rain gauge data set embraces records from 6471 stations (Figure 2) each of which covers at least part of the 15-year study period. Roughly 5000 observations are available per day. The interstation distance of the network varies between 10 and 25 km over most parts of the domain, while there is a slightly inferior coverage in some areas to the south of the ridge (e.g., central and western Po valley, Adriatic coast) (see Figure 2). The database includes observations from all national high-resolution networks in the Alpine region and was assembled from numerous data portions that have been kindly provided by the meteorological and hydrological services. A complete listing of the data sources and details of the rain gauge data set are given by *Frei and Schär* [1998].

[12] The spatial analysis of the rain gauge observations onto the regular grid was undertaken with the intention that an analysis value should represent an estimate of area-mean precipitation in the 50×50 km^2 surrounding of the analysis grid point (i.e., the model grid box). This procedure ensures compatibility of spatial representativity between the observational fields and the regional models and hence avoids spurious differences in the statistics emanating from incompatible resolution [see *Mearns et al.*, 1995; *Osborn and Hulme*, 1997]. A modified version of the Synagraphic

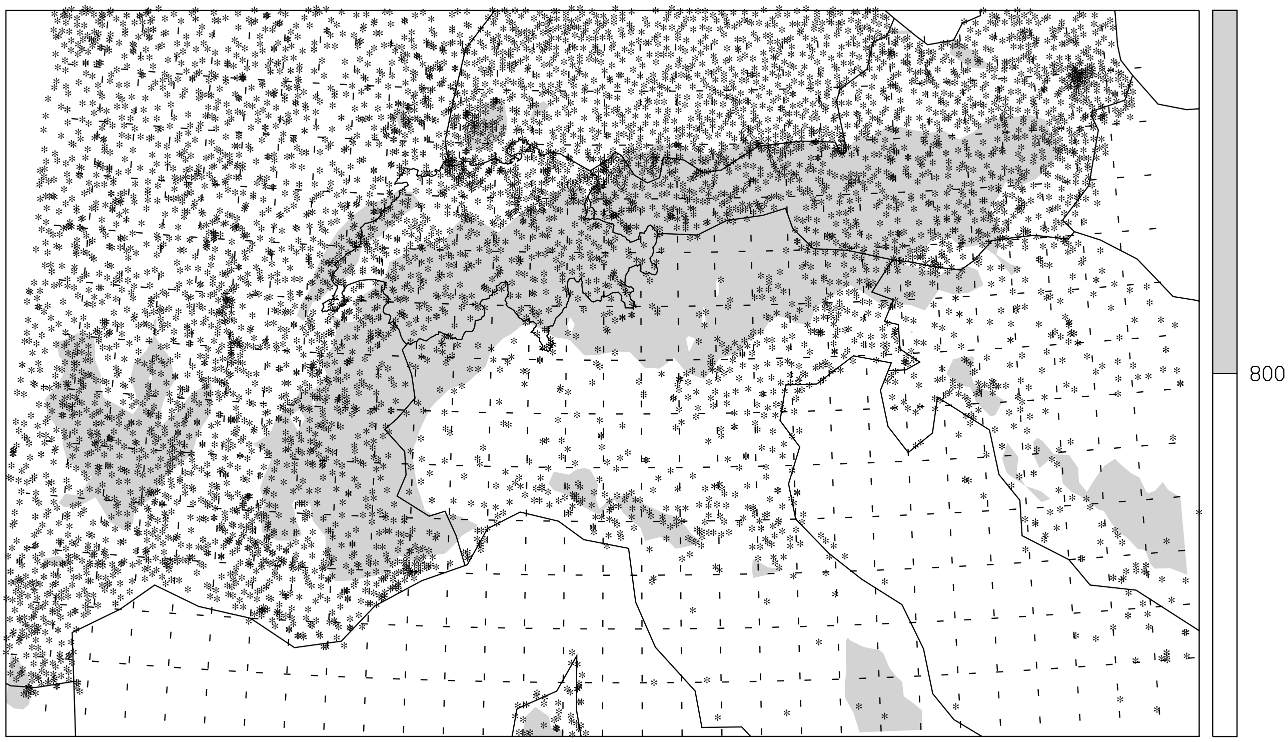

Figure 2. Rain gauge stations from which precipitation records have been used for the daily observational analysis (OBS). Dashed lines represent common analysis/model grid used for the evaluation.

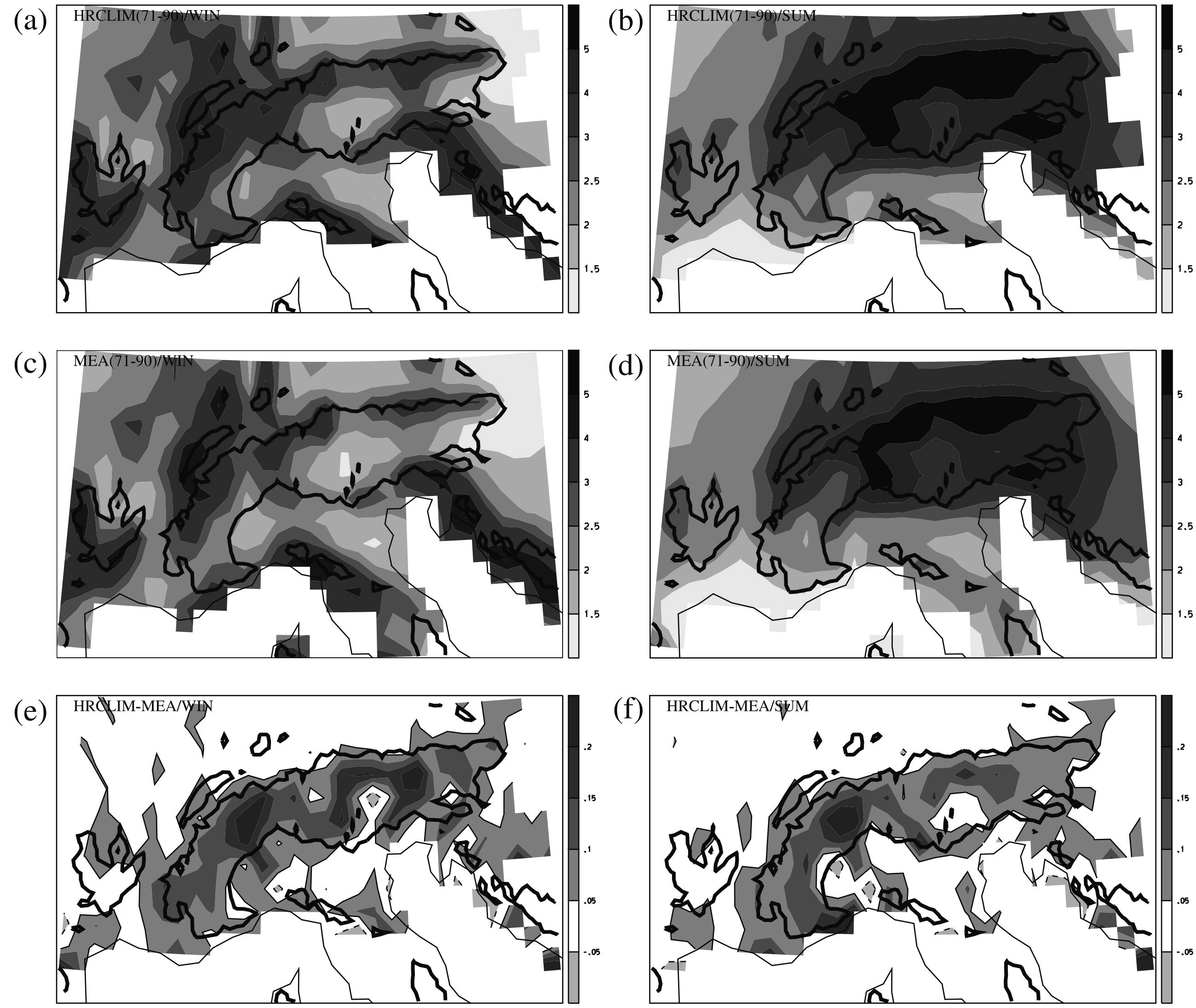

Figure 3. Mean precipitation (in mm/d) from an aggregated high-resolution climatology (panels a and b) for which the network bias was corrected [*Schwarb et al.*, 2001] (reference period 1971–1990) and from the analysis used in the present study (panels c and d) but the same reference period as the high-resolution climatology. Panels e and f: Relative difference between the two analyses in fractions of panels a and b. Panels a, c, and e for winter (DJF) and b, d, and f for summer (JJA).

Mapping System (SYMAP) algorithm [*Shepard*, 1984; see also *Willmott et al.*, 1985] was employed for the spatial analysis. The algorithm combines weighting schemes that account for distance from and directional clustering of stations around the analysis grid point. Except for the resolution, the procedure is similar to that employed for an earlier analysis with the same data set (25 km resolution) [*Frei and Schär*, 1998]. In the present application between 10 and 50 station observations contribute to the analysis at each grid point. The analysis was applied on a daily basis and resulted in a continuous data set of daily Alpine precipitation fields, which will be referred to as OBS in the text.

2.3. Errors and Uncertainty of the Observation Reference

[13] Several sources of error and uncertainties in the analysis are relevant for the interpretation of evaluation results:

[14] In the region of the main Alpine ridge, the distribution of rain gauges is biased, with high-elevation areas being undersampled in comparison to lowland and valley-floor conditions [e.g., *Frei and Schär*, 1998]. The magnitude of this *network bias* was estimated by comparing the present analysis with a high-resolution climatology [*Schwarb et al.*, 2001], which was constructed with additional monthly totalisor data at high elevations, and using an analysis technique that compensates for representation biases in the station sample [see also *Daly et al.*, 1994]. The comparison (Figure 3) suggests that the network bias of the present analysis is largely confined to the main ridge (i.e., high elevations) where it attains values up to 25% for a few 50×50 km^2 grid pixels. Nevertheless, the magnitude of the network bias is smaller than the gross variations across the ridge as is evident in the similarity of patterns between the aggregated high-resolution climatology and the analysis used in this study (cf. panels a and c and b and d in Figure 3). In the mean

Table 1. Estimates of Precipitation Bias (Underestimate) in the Alpine Analysis Due to Measurement Bias and Network Bias

	Measurement Bias[a]			Domain Mean Bias[b]		
	<600 (62%) (%)	600–1500 (34%) (%)	>1500 (4%) (%)	Measurement Bias (%)	Network Bias (%)	Total (%)
Winter	8	12	40	11	5	16
Spring	5	10	25	7	4	11
Summer	4	8	12	6	4	10
Autumn	5	10	25	7	4	11

[a]Typical values for height zones (mMSL) [*Sevruk*, 1985; *Richter*, 1995].
[b]Domain mean bias is for domain AL (see Figure 1a).

of the Alpine domain (domain AL in Figure 1a) the comparison reveals lower mean precipitation in the present analysis by 5% in winter and by 4% in summer. Hence the network bias is a relevant factor for a quantitative assessment of mean precipitation over the domain, but it is unlikely to affect the gross spatial variations represented by OBS.

[15] Wind field deformation and deflection of hydrometeors over the gauge orifice results in a systematic *measurement bias* [e.g., *Neff*, 1977; *Groisman and Legates*, 1994; *Nespor and Sevruk*, 1999]. Estimates of this error for the Alpine region [see *Sevruk*, 1985; *Richter*, 1995] are largest in winter (high wind speed, high fraction of snowfall) when the undercatch is about 8% below 600 mMSL and around 40% above 1500 mMSL. For summer the undercatch varies between 4% at low and 12% at high-altitude stations. (Note that the bias depends on the station's wind exposure. These values represent typical measures of the bias.)

[16] The network and measurement biases are taken into account in the discussion of the results for domain mean precipitation statistics in section 4. For this purpose, an ad hoc estimate of the domain mean bias is given in Table 1. It is obtained from a weighted average of the literature values for rain gauge undercatch [*Sevruk*, 1985; *Richter*, 1995], using the height distribution of the Alpine rain gauges, and from the mean network bias, estimated by comparison to the *Schwarb et al.* [2001] high-resolution climatology. We estimate that OBS underestimates domain mean precipitation by 16% and 10% in winter and summer respectively and by 11% in spring and autumn. These estimates are consistent with a recent comparison of the multiyear water balance (runoff minus evaporation) in mesoscale Alpine catchments with conventional precipitation climatologies [*Schädler and Weingartner*, 2002]. As a first approximation we assume that these values also represent the seasonal biases for precipitation intensity and the quantiles of the frequency distribution. (Actually, the bias will be slightly higher (lower) for low (high) quantiles because the rain gauge undercatch depends on hydrometeor size and hence on precipitation intensity.)

[17] An additional uncertainty in our evaluation is posed by the fact that the grid spacing of the climate models varies slightly (50–70 km), and that the effective resolution of the climate models can differ from their actual grid spacing. The effective resolution of precipitation processes depends for example on the degree of numerical diffusion and on the actual resolution of the topography. For some of the models in this study the topography was filtered from two-grid waves and therefore its effective resolution is coarser than the grid spacing. Again, it has been argued that the concepts of convective parameterization in numerical models are based on processes that are of a smaller scale than the grid spacing itself and hence simulated precipitation statistics could be representative of scales smaller than the models' grid spacing [e.g., *Skelly and Henderson-Sellers*, 1996]. As a result, the effective resolution of precipitation in numerical models is unknown, and there is some uncertainty as to how the effective resolution (i.e., the aggregation scale) of the observational reference should be chosen to be compatible with that of the models. To account for this scale uncertainty in the high-frequency precipitation statistics of OBS, several analyses of the daily rain gauge observations were carried out: Apart from the standard 50 km aggregation, two additional analyses were derived using aggregation scales of 40 and 100 km. The results from the three analyses define a reasonable range of the observed statistics against which the model results can be compared.

2.4. Statistics of Daily Precipitation

[18] Several climatological statistics of daily precipitation (quantities characterizing the distribution function of daily precipitation) have been calculated from the simulated precipitation fields and from the observational analyses for each month of the year. These include mean daily precipitation (MEA), the frequency of wet days (FRE), the mean precipitation intensity (INT, mean amount per wet-day) and a series of empirical quantiles of the distribution of wet-day amounts (Qxx). Acronyms and definitions of the statistics are listed in Table 2. As threshold for the discrimination between wet and dry days a value of 1 mm was chosen. In comparison to smaller values (e.g., 0.1 or 0.5 mm) this choice makes the evaluation less sensitive to the measurement/observer accuracy and to the tendency of some models to produce excessive occurrence of very weak precipitation.

[19] For optimal consistency in the evaluation, the statistics has been calculated using a common diagnostic software for all the models and the observations. The calculation was undertaken for each month of the year and for each model/observation grid box. Hence the statistics are based on a sample size of 450 daily values (15

Table 2. Statistics of Daily Precipitation Diagnosed From Model Integrations and From the Daily Gridded Analysis

Statistic	Definition
MEA	mean precipitation (mm/d)
FRE	frequency of days with precipitation $\geq$1 mm (wet-day frequency, fraction)
INT	mean amount per wet day (precipitation intensity, mm/d)
Qxx	quantiles of distribution function of wet-day amounts (mm/d), xx = 20%, 40%, 50%, 60%, 80%, 90%, and 95%

Table 3. Summary of Grid Configurations and Parameterizations for the RCMs

Model	Resolution $nx \times ny$	Nudging Zone (Number of Points)	Number of Levels	Convection	Microphysics	Land Surface	Radiation
ARPEGE	50–70 km (over Europe), global model	–	31	Mass flux, *Bougeault* [1985]	Statistical and diagnostic, *Ricard and Royer* [1993]	ISBA 4 thermal and 2 moisture layers *Douville et al.* [2000]	*Mocrette* [1990]
CHRM	0.5° (55 km), 81 × 91	8, *Davies* [1976]	20	Mass flux, *Tiedtke*, [1989]	*Kessler* [1969], *Lin et al.* [1983]	4 thermal and 3 moisture layers, *Dickinson* [1984], *Jacobsen and Heise* [1982]	*Ritter and Geleyn* [1992]
HadRM	0.44° (50 km), 106 × 111	4	19	Mass flux, *Gregory and Rowntree* [1990], *Gregory and Allen* [1991]	*Smith* [1990], *Jones et al.* [1995]	4 thermal and 4 moisture layers, *Cox et al.* [1999]	*Edwards and Slingo* [1996]
HIRHAM	0.44° (50 km), 110 × 104	10 (no vertical dependence), *Davies* [1976]	19	Mass flux, *Tiedtke* [1989], *Nordeng* [1994]	*Sundqvist* [1988]	5 thermal layer, 1 moisture bucket, *Dümenil and Todini* [1992]	*Morcrette* [1991], *Giorgetta and Wild* [1995]
REMO	0.5° (55 km), 81 × 91	8, *Davies* [1976]	20	Mass flux, *Tiedtke* [1989], *Nordeng* [1994] for CAPE closure	*Sundqvist* [1978]	5 thermal layer, 1 moisture bucket, *Dümenil and Todini* [1992]	*Morcrette* [1989], *Giorgetta and Wild* [1995]

years, 30 days/month), which allows for robust estimates. Even in the worst case, with a precipitation frequency of 0.2 (occurring in summer months at a few grid points along the Mediterranean coast), the largest quantile Q95 is still exceeded on 4 days during the 15-year period.

[20] The evaluation of section 4 embraces the mean annual cycle of the statistics averaged over a subdomain and the spatial distribution of the statistics averaged over the months of a season. Distribution functions of daily precipitation are derived from spatial averages of the quantiles over the Alpine subdomain.

3. Regional Climate Models

[21] The evaluation and intercomparison involves the most recent versions of five regional climate models (RCMs) developed and operated at climate modeling centers across Europe. Except for one variable-resolution global climate model (ARPEGE), all models are limited area models (LAMs) with atmospheric forcing at their lateral boundaries.

[22] Table 3 summarizes the grid configurations and major parameterization packages used by the various regional climate models. (Details for each of the models are given in the subsections below.) The computational domain is comparable between the limited area models and covers sections of the western North Atlantic and the European continent (see Figure 4). The region of the European Alps is located close to the center of the domains and is well separated from the models' lateral boundary zones. The models exhibit a resolution of 50–70 km in this area.

[23] The simulations considered in this study were forced along the observed evolution of the atmosphere and the sea surface temperature over the 15 years (1979–1993). In the case of the LAMs, boundary conditions were taken from the ECMWF reanalyses (ERA15) [*Gibson et al.*, 1999], while the ARPEGE simulation corresponds to an AMIP-type integration with prescribed sea surface temperature and sea ice from observations for the same period. The procedure of "perfect" boundary conditions employed for the LAMs ensures that the present evaluation is primarily reflecting errors of the RCMs themselves, and not the effect from errors in the large-scale forcing as it would in the case of forcing from a free GCM [e.g., *Christensen et al.*, 1998; *Machenhauer et al.*, 1998]. The domain size used with the LAMs is small enough to ensure that the boundary conditions exert strong control over the circulation in the model interior [*Jones et al.*, 1995; *Jacob and Podzun*, 1997] and large enough that the domain interior is not contaminated by the lateral boundaries [*Warner et al.*, 1997]. The models' settings have been demonstrated to reproduce the observed day-to-day evolution of midtropospheric circulation fields during seasons of significant synoptic-scale forcing [e.g., *Christensen et al.*, 1997; *Lüthi et al.*, 1996; *Jacob et al.*, 2001].

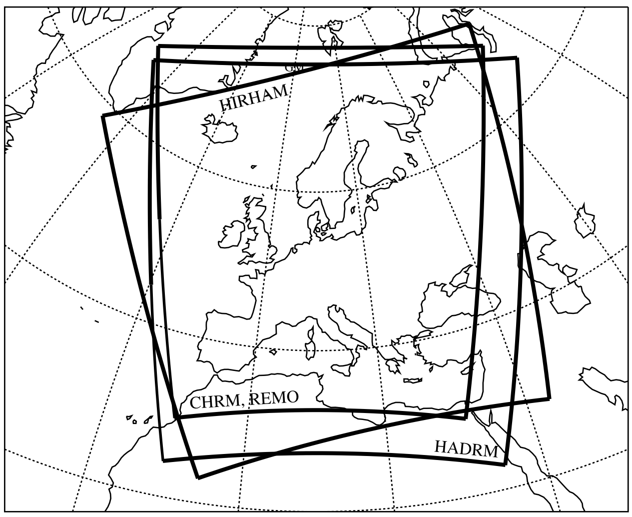

Figure 4. Computational domain (including the lateral nudging zone) of the limited area regional climate models. Domains for CHRM and REMO are identical. (ARPEGE is a global model.)

[24] The ARPEGE model does not have the same circulation constraints as the four RCMs and therefore the evaluation results on this model are not strictly comparable to those of the RCMs. AGCM experiments have demonstrated that, in the extratropics, the deterministic control of sea surface temperature and sea ice on interannual variations of surface pressure and precipitation is limited [*Lau et al.*, 1997; *Gates et al.*, 1999] and that the atmosphere–land component of the climate system contributes a significant fraction of the magnitude of interannual variability [*Hansen et al.*, 1997]. Therefore the performance of ARPEGE in the Alps is also affected by lack of predictability, which may not be interpreted as systematic model error. Moreover the results of ARPEGE can be influenced by the representation of the large-scale circulation [*Déqué and Piedelievre*, 1995], which is simulated in ARPEGE but prescribed for the RCMs.

[25] For two of the climate models (CHRM and REMO) the prognostic soil parameters (temperature and moisture content) are initialized directly by interpolation from the driving reanalysis ERA15. This procedure involves the possibility of an initial imbalance with the particular model's soil scheme and an associated spin-up period for the model soils. For ARPEGE and HIRHAM the initial soil values were taken from a 1-year preintegration of year 1979 and HadRM was initialized from the corresponding atmospheric GCM to adjust/optimize soil balances at integration start. An eventual soil spin-up may affect the first few months of the model integrations depending on the magnitude of the imbalance, however diagnosis of the soil evolution for the models suggests that this period is not lasting longer than one integration year [see also *Christensen*, 1999] and therefore only marginally affects the 15-year mean precipitation statistics.

3.1. ARPEGE

[26] ARPEGE-IFS is a global operational forecast model in use at ECMWF and at the French Meteorological Service with different physical parameterizations. A third version is used for climate simulations with another parameterization set. This version is run with variable horizontal resolution, from 50 km in the center of the Mediterranean Sea to 450 km in the southern Pacific Ocean. It has 31 vertical levels in hybrid coordinate. An earlier version has been described by *Déqué et al.* [1998]. The new features are the radiation and the cloud-precipitation-turbulence scheme (see Table 3). The convection scheme is a mass flux scheme with moisture convergence closure. Soil moisture was initialized by interpolating an ECMWF winter analysis and running a full annual cycle to get rid of initial conditions. A 1-year cycle is considered to be sufficient for the ISBA scheme to adjust (at least in midlatitudes where vegetation is efficient enough to empty the root reservoir in a few months).

3.2. CHRM

[27] The limited area model CHRM derives from the operational weather forecasting model HRM of the German and Swiss meteorological services [*Majewski*, 1991], which has been adapted into a climate version by ETH Zürich [*Lüthi et al.*, 1996; P. L. Vidale et al., Predictability and uncertainty in a Regional Climate Model, submitted to *Journal of Geophysical Research*, 2002, hereinafter referred to as Vidale et al., submitted manuscript, 2002]. The model's computational grid is a regular latitude/longitude grid with a rotated pole, a resolution of 0.5° (about 55 km) and 20 vertical levels in hybrid coordinates. The model has a full package of physical parameterizations (see Table 3). Recent changes in relation to previous model versions [see also *Schär et al.*, 1999; *Heck et al.*, 2001] consist in the use of an updated version of the Biosphere–Atmosphere Transfer Scheme (BATS) [*Dickinson*, 1984], including a module for the freezing of soil moisture, deeper soils and corresponding soil bottom boundary conditions and the *Beljaars and Viterbo* [1998] surface layer parameterization. The lateral boundaries are updated every 6 hours (with linear interpolation in between). The soil profiles are initialized from ERA15, retaining a "climatological" deep layer, which acts as a fixed boundary condition, but is only accessed in case the root zone layer dries further than the air dryness point (ADP). A detailed description of the model version used in this study and further evaluations of the integration are given by Vidale et al. (submitted manuscript, 2002). CHRM and REMO (see below) share the same dynamical core, but they differ in terms of physical parameterizations.

3.3. HadRM

[28] HadRM is the most recent Hadley Centre regional climate model HadRM3H (R. G. Jones et al., manuscript in preparation, 2003). It is a limited area higher-resolution version of the AGCM HadAM3H (J. M. Murphy et al., manuscript in preparation, 2003, hereinafter referred to as Murphy et al., manuscript in preparation, 2003) which itself is an improved version of HadAM3, the atmospheric component of the latest Hadley Centre coupled AOGCM, HadCM3. HadAM3 is described by *Pope et al.* [2000] and contains all the usual representations of atmospheric and land surface physics (see Table 3). The modifications of relevance here (as they relate to precipitation and were instrumental in reducing a warm and dry summer bias) are as follows: (1) A scheme to treat the radiative effects of anvil cirrus in deep convective regimes is included [*Gregory*, 1999]. (2) The threshold relative humidity for cloud formation within a grid box has been parameterized as a function of horizontal variability resolved by the climate model [*Cusack et al.*, 1999]. (3) An empirically adjusted cloud fraction parameterization has been introduced which sets the cloud fraction to 0.6 rather than 0.5 when the grid box specific humidity reaches saturation (Murphy et al., manuscript in preparation, 2003). Soil moisture was initialized from a HadAM3 simulation of the present-day climate using the December conditions from an arbitrary year in the integration. These data were representative of average wintertime soil moisture values.

3.4. HIRHAM

[29] The HIRHAM applied in this study is an updated version of HIRHAM4 [*Christensen et al.*, 1996]. The dynamical part of the model is based on the hydrostatic limited area model HIRLAM, documented by *Machenhauer* [1988] and *Källén* [1996]. Prognostic equations exist for the horizontal wind components, temperature, specific humidity, liquid water content and surface pressure. HIRHAM4 uses the physical parameterization package of the general circulation model ECHAM4, developed by *Roeckner et al.* [1996]. These parameterizations include radiation, land surface pro-

cesses, sea surface sea ice processes, planetary boundary layer, gravity wave drag, cumulus convection and stratiform clouds. The treatment of precipitation processes includes a newly introduced low precipitation threshold that reduces so-called drizzling, and only when convection is absent. This modification has improved the annual cycle of the mean precipitation in general [e.g., *Hagemann et al.*, 2001], but also more specifically precipitation frequencies over Denmark [*Christensen et al.*, 2001b]. The present work is part of the further validation. The land surface parameterization uses five prognostic temperature layers and one bucket moisture layer. Runoff is calculated within the Arno scheme [*Dümenil and Todini*, 1992]. Moreover, the updated model utilizes high-resolution data sets of land surface characteristics [e.g., *Hageman et al.*, 1999; *Christensen et al.*, 2001c]. The standard procedure to initialize soil moisture in the model for climate simulations is a cyclic repetition of the first model year (i.e., 1979 in the present integration) basically following the procedure of *Christensen* [1999]. However, in contrast to the model of *Christensen* [1999], the model starts from relatively moist initial conditions. It is assumed that the first cyclic year is sufficient to obtain a balanced initial state for January 1979. The adopted computational grid is a rotated regular latitude/longitude grid (110 × 104 grid points) with the rotated South Pole at (27°E, 37°S), a resolution of 0.44° (about 50 km) and 19 vertical levels in hybrid sigma-p coordinates.

3.5. REMO

[30] The regional climate model REMO [*Jacob*, 2001], as used for the present study, is a combination of the dynamical core of the Europamodell/Deutschlandmodell of the German Weather Service [*Majewski and Schrodin*, 1994] and the physical parameterization schemes of the ECHAM4 global climate model [*Roeckner et al.*, 1996] of the Max-Planck Institute of Hamburg. REMO uses a spherical Arakawa-C grid on regular latitude–longitude coordinates with a rotated pole and a resolution of 0.5° (about 55 km). 20 vertical levels are used. The integration domain covers the whole of Europe and parts of the Atlantic Ocean. Soil moisture is initialized by interpolation of values from the driving ERA15 on 1 January 1979. REMO has the same dynamical core like CHRM and shares the same physical parameterization schemes like those in HIRHAM, however a few minor changes have been introduced in both parts.

4. Results

[31] Results of the evaluation of daily precipitation statistics in the Alpine region are presented sequentially for the annual cycle of the domain mean conditions (section 4.1), the spatial distribution of some of the statistics for the winter and summer seasons (section 4.2) and for the empirical distribution function (section 4.3). The last section (section 4.4) compares the model results for several other European regions in order to assess if the intermodel differences evident in the Alpine region are specific to that region or more general features.

4.1. Annual Cycle

[32] Figure 5 displays the annual cycle of mean precipitation (MEA), wet-day frequency (FRE), precipitation intensity (INT) and the 90% quantile of the wet-day amount (Q90). The model biases for each of the statistics in winter (DJF) and summer (JJA) are listed in Table 4. Values represent domain mean conditions over the Alpine subdomain (AL) (see Figure 1a), and grid points for which observations are missing (e.g., the Adriatic Sea) were also excluded from the model fields. The shading for OBS represents the scale uncertainty (see section 2.3). The ad hoc correction of the measurement and network biases in the observations (see Table 1) is included in Table 4 but not in Figure 5.

[33] For mean precipitation (MEA, Figure 5a) the models follow qualitatively the main characteristics of the observed annual cycle with wet conditions in spring and early summer and dry conditions in late winter (especially February) and midsummer (especially July). Many of the models however tend to overestimate the amplitude of the annual cycle, showing excessive dryness in late summer and early fall. For CHRM, HadRM and REMO the underestimate is as large as 35% in August and September. Table 4 lists the seasonal bias of the statistics when the systematic precipitation bias of OBS is corrected by the estimates of Table 1. For MEA, the bias varies between −23% and +3% in winter and between −27% and −5% in summer. For most of the models the bias is the lowest in spring and the largest in autumn.

[34] The comparison for wet-day frequency and precipitation intensity (see Figures 5b and 5c) reveals considerable intermodel differences. ARPEGE and HIRHAM both overestimate the FRE and at the same time underestimate precipitation intensity through most of the year. The model results are well outside the range defined by an effective resolution of 40–100 km in the observations (shaded area). The bias is most prominent in summer, when these two models produce 40–60% more wet days and a 40% lower intensity than observed (Table 4). The biases in frequency and intensity mutually compensate and do not reflect in more substantial errors in mean precipitation by these two models, in fact the dry bias of MEA in summer is considerably smaller than for the other models. On the other hand, CHRM, HadRM, and REMO depict realistic values of wet-day frequency and much smaller underestimates in precipitation intensity from late autumn to early summer (Figures 5b and 5c). (Note that the high precipitation intensity of HadRM for winter is very realistic when the observation bias is corrected (Table 4).) However, in the late summer season these models underestimate both the frequency and intensity (though to a lower extent than the other models). A close inspection (see Table 4) reveals that the excessive summer dryness is primarily associated with underestimates in the intensity for HadRM and REMO whereas a combination of errors in both quantities contributes to the summer dryness of CHRM.

[35] The annual cycle in Alpine heavy precipitation (as revealed by Q90) (see Figure 5d) exhibits a prominent peak in September and October. During this time of the year particularly heavy events occur along the southern rim of the Alps, which are characterized by the advection of moist air masses from the Mediterranean, orographic lifting along the southern rim, and embedded convection [e.g., *Massacand et al.*, 1998; *Buzzi and Foschini*, 2000; *Stein et al.*, 2000]. All RCMs are reproducing this autumn peak in Q90,

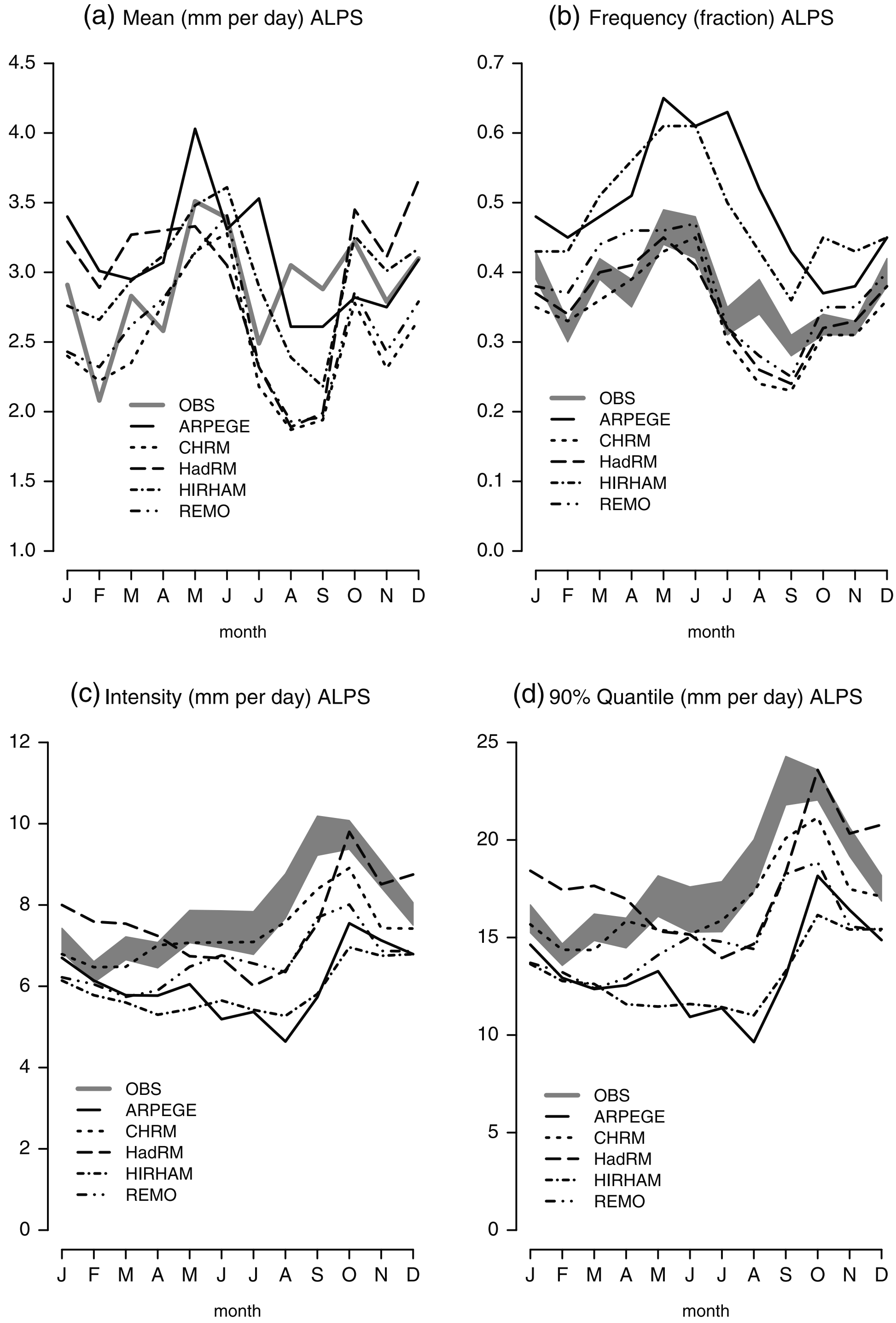

Figure 5. Annual cycle of precipitation statistics averaged over the Alpine region (2.25°–17.25°E, 44.25°–48.75°N, grid points with missing values in observations excluded). (a) Mean precipitation (MEA, mm per day); (b) wet-day frequency (FRE, fraction); (c) precipitation intensity (INT, mm per day); (d) 90% quantile of wet-day amounts (Q90, mm per day). Shaded area for OBS represents the range of results expected from effective model resolutions between 40 and 100 km (scale uncertainty, see section 2.3).

which attests the models' capability to capture the most prominent seasonal feature of heavy precipitation in the Alps. In quantitative terms however, all models underestimate Q90 during the entire summer half-year (in JJA the bias varies from −46% to −18%) (Table 4) and the autumn peak is delayed in ARPEGE, HadRM and HIRHAM. Notice that the general tendency to underestimate the 90% quantile is in line with the general underestimate of precipitation intensity.

4.2. Spatial Distribution

[36] Figure 6 depicts the spatial distribution of mean precipitation for winter (DJF) of all five models and the observations (upper left panel). The models reveal good

Table 4. Bias and Spatial Correlation of Model Precipitation Statistics (see Table 2) in the Alpine Region (Domain AL)[a]

		DJF		MAM		JJA		SON	
Statistic	Model	Bias (%)	Corr	Bias (%)	Corr	Bias (%)	Corr	Bias (%)	Corr
MEA	ARPEGE	1	0.62	0	0.43	−5	0.78	−17	0.40
	CHRM	−23	0.62	−18	0.67	−26	0.80	−29	0.63
	HadRM	3	0.65	−2	0.63	−27	0.75	−14	0.53
	HIRHAM	−8	0.62	−5	0.58	−10	0.80	−14	0.42
	REMO	−20	0.56	−15	0.47	−23	0.81	−27	0.40
FRE	ARPEGE	27	0.88	35	0.72	58	0.85	28	0.68
	CHRM	−5	0.84	−2	0.70	−11	0.91	−8	0.73
	HadRM	0	0.72	4	0.69	−11	0.85	−3	0.68
	HIRHAM	20	0.79	39	0.65	39	0.86	36	0.66
	REMO	5	0.80	13	0.64	−4	0.89	3	0.68
INT	ARPEGE	−22	0.62	−28	0.44	−42	0.40	−36	0.66
	CHRM	−18	0.63	−15	0.75	−16	0.62	−23	0.72
	HadRM	−4	0.64	−12	0.66	−27	0.26	−19	0.62
	HIRHAM	−26	0.47	−33	0.67	−37	0.48	−39	0.63
	REMO	−24	0.63	−25	0.73	−25	0.46	−29	0.74
Q90	ARPEGE	−25	0.71	−31	0.48	−46	0.31	−36	0.63
	CHRM	−16	0.65	−17	0.74	−18	0.63	−21	0.69
	HadRM	0	0.69	−9	0.68	−26	0.29	−17	0.67
	HIRHAM	−26	0.52	−35	0.67	−42	0.28	−39	0.62
	REMO	−25	0.66	−28	0.73	−25	0.43	−29	0.73

[a]Measurement and network biases are corrected in observed MEA, INT, and Q90 according to Table 1.

qualitative correspondence with the gross regional distribution. Correlations of the simulated with the observed pattern are around 0.6 and vary little between models (Table 4). The models reproduce the pattern of wet conditions along the northwestern rim of the ridge and in some cases also those centered over the smaller-scale hill ranges to the north of the main ridge (Jura, Black Forest, and Vosgues). The models differ with regard to spatial variance with HadRM showing the most variable and REMO the smoothest patterns. Some of these differences may be due to differences in the effective resolution of the model topography and differences in the degree of numerical diffusion. However, there is a tendency of ARPEGE and HadRM toward too dry conditions in the Po valley and the Lower Rhone valley which could also hint to excessive rain shadowing in the lee of the topographic barriers, which for these models exhibit strong precipitation enhancement.

[37] Again the gross patterns of wintertime wet-day frequency (Figure 7) and precipitation intensity (Figure 8) are reproduced by the models, with correlations around 0.8 for FRE and 0.6 for INT. Note for example the prominent gradient of FRE across the main ridge of the Alps and the Massif Central. Major discrepancies are however found in the magnitude of precipitation frequency to the north, which is overestimated, not only, but especially by ARPEGE and HIRHAM. In ARPEGE the overestimate is confined to the north of the ridge, while it is also evident for the south in HIRHAM. These two models also depict less clearly the observed north to south increase of precipitation intensity, a feature that is reproduced qualitatively by the other models.

[38] The corresponding results for the summer season (Figures 9–11) reveal a series of interesting features: First, all models successfully reproduce the winter to summer shift of the moist anomaly from the western to the eastern sector of the ridge (Figure 9). This shift reflects the different nature of precipitation with a prominence of topography related convection over the ridge in summer and frontal disturbances approaching from the west in winter [e.g., *Schär et al.*, 1998]. Second, the underestimation of summer mean precipitation found for CHRM, HadRM and REMO has a different background: While HadRM and REMO have primarily too dry conditions on the southern parts of the area (Po valley, Mediterranean coast), CHRM underestimates the value, spatial extent and precipitation intensity of the moist anomaly over the ridge (Figures 9 and 11). Thirdly, ARPEGE and HIRHAM exhibit too high wet-day frequency and too low precipitation intensity (Figures 10 and 11). These errors are domain wide, they are larger in magnitude than in winter, and they mutually cancel to yield reasonable values and distributions for mean precipitation. Finally, it is noteworthy that the most prominent intermodel differences and deviations from observations are found in the distribution for summer precipitation intensity (Figure 11). For example, the observed anomalies of high intensity along the southern rim of the ridge are poorly represented by all the models. Values of spatial correlation are mostly

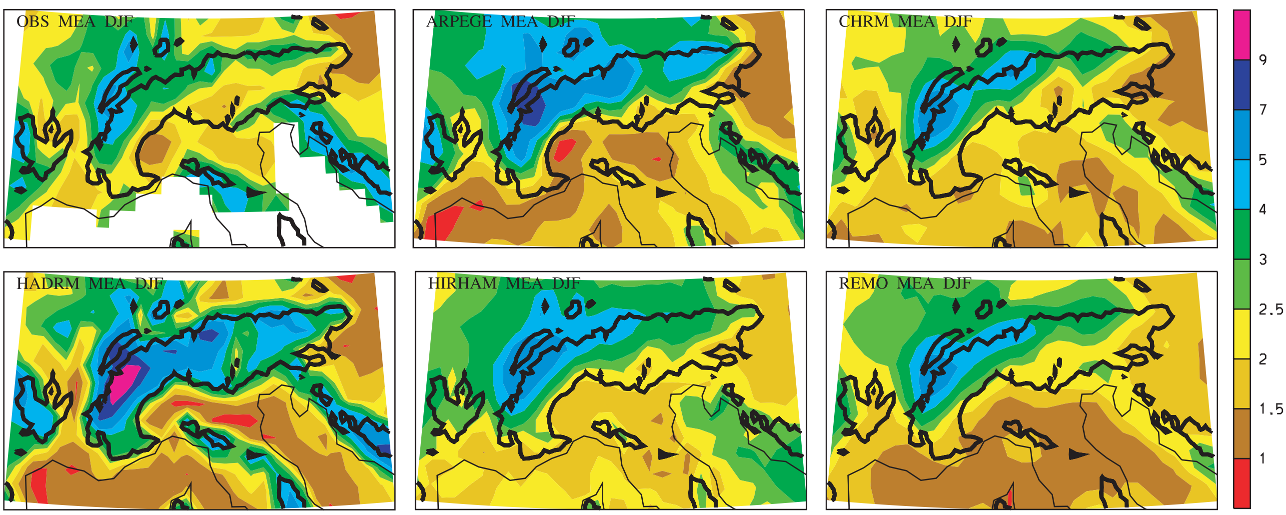

Figure 6. Mean winter (DJF) precipitation (MEA, mm/d) for OBS (top left) and models.

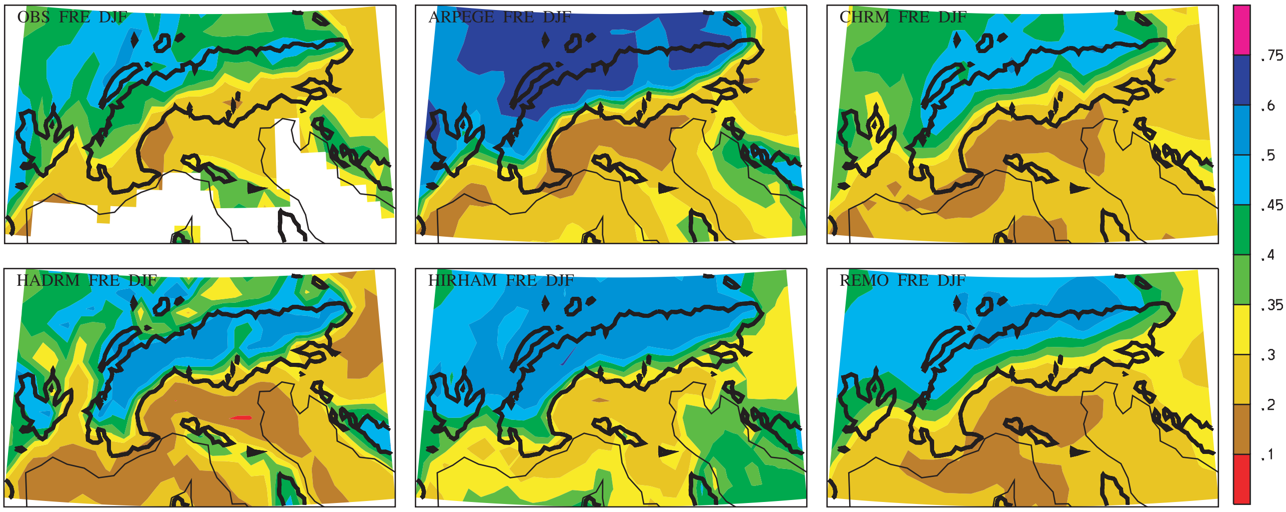

Figure 7. Mean winter (DJF) precipitation frequency (FRE, fraction) for OBS (top left) and models.

lower than 0.5, significantly lower than for any other season (Table 4).

[39] It is of special interest to evaluate the models' representation of heavy daily precipitation. Here we focus on autumn (SON), the main season of heavy precipitation activity in the Alpine region (cf. Figure 5d) [*Frei and Schär*, 1997]. Figure 12 depicts the distribution of the 90% quantile (Q90) conditional on wet days. The observations reveal three distinct regions where Q90 exceeds 50 mm (SE of the Massif Central, south central Alps and north of Adriatic Sea). Although these anomalies are of limited spatial extent (i.e., span over a few model grid points only), some of the models reveal distinct signals of these narrow features. The correlation between the observed and simulated pattern is around 0.65 (Table 4). On the scale of the entire domain, however, Q90 is underestimated by the models (see also Figure 5d) and this reflects systematic biases in the distribution function, as will be shown later. Despite the substantial biases the reproduction of the regional patterns (at least by some of the models) is encouraging when we recognize that the hot spots are related to topographic mechanisms (e.g., regional channeling of southerly moist airflows), which are near the limit of the model resolution and complex, i.e., not merely resulting in a simple elevation dependence of precipitation.

[40] The simulated patterns of Q90 for winter and spring (not shown) shows a similarly satisfying correspondence with OBS (see correlations in Table 4). However, for summer the distribution reveals more significant deviations. The correlation drops to values below 0.4 for most of the models. Heavy precipitation during this time of the year is associated to convective activity and its spatial distribution is determined by thermal topographic triggering mechanisms, which, apparently, are more difficult to reproduce, by the models in comparison to the dynamical effects of the ridge dominating in the other seasons.

4.3. Distribution Function

[41] An evaluation of the cumulative distribution function of daily precipitation (i.e., the frequency of excess as a function of threshold) is provided in Figure 13. The distribution functions are determined from the domain mean

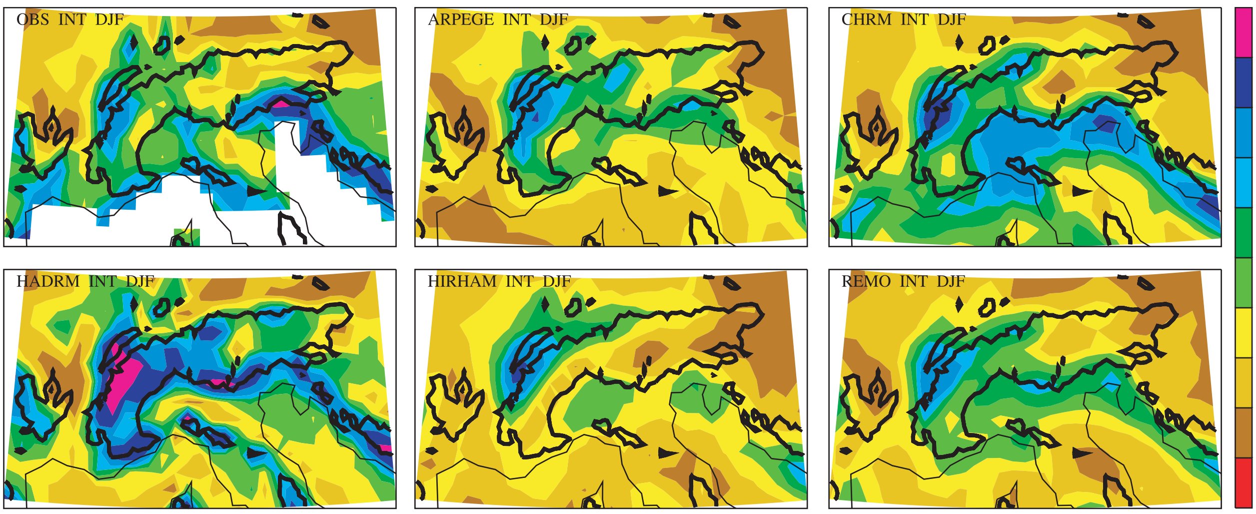

Figure 8. Mean winter (DJF) precipitation intensity (INT, mm/d) for OBS (top left) and models.

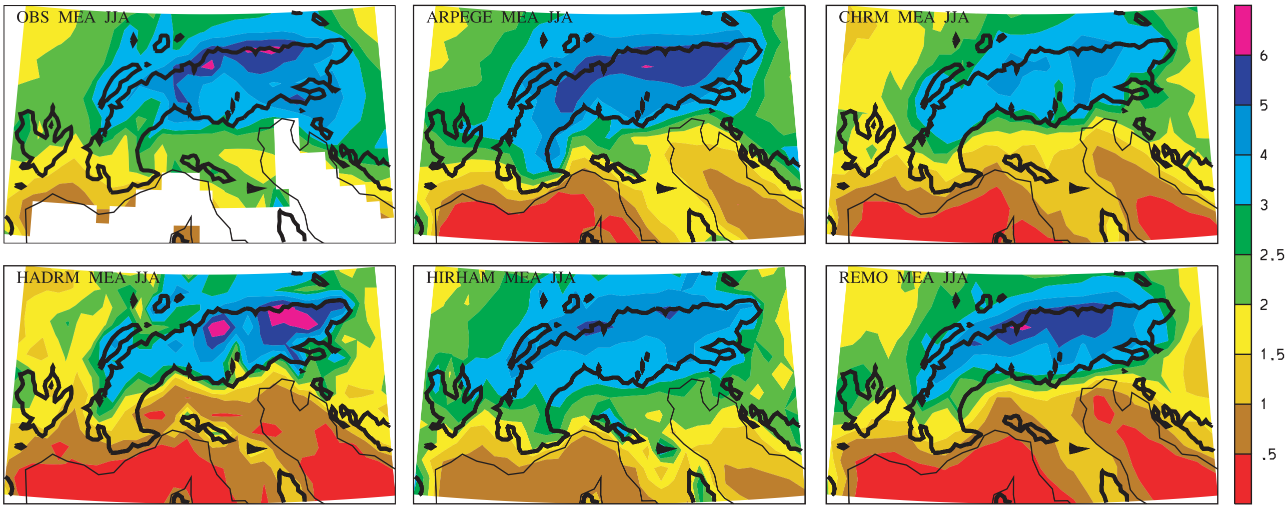

Figure 9. Mean summer (JJA) precipitation (MEA, mm/d) for OBS (top left) and models.

values of the evaluated quantiles (see Table 2). Hence they represent the domain mean of distribution functions for individual grid boxes, not the distribution function of daily domain mean precipitation. As with the previous evaluation for FRE and INT, several distribution functions are determined for OBS using aggregation scales of 40 and 100 km. These distributions delimit the uncertainty of the unknown effective model resolution and are depicted in shades.

[42] The frequency distributions expressed relative to the total number of days (i.e., including wet and dry days in the diagnostics) are depicted in Figures 13a–13d for all four seasons. In winter, there is qualitative agreement with the observations though all models exhibit deviations from the observed distribution that cannot be explained solely by the uncertainty of effective resolution: HadRM overestimates the excess frequency beyond a threshold of about 7 mm and hence its distribution function has a longer tail than all other models. This behavior is likely associated with the overestimation of topographic precipitation enhancements evident in the spatial distribution of INT (Figure 8). Conversely CHRM underestimates the excess frequency at low but performs well at high thresholds. As regards the two models with overestimates in wet-day frequency, the distribution function reveals, that this overestimate is confined to low-intensity events (smaller than 4 mm/d) in HIRHAM but prevails to moderate intensities (till 13 mm/d) in ARPEGE.

[43] In summer (Figure 13c) all models tend to underestimate the frequency of intense and heavy precipitation. The biases at high thresholds are considerable in magnitude and reveal in a too steep gradient of the distribution functions compared to observations. Most of the models fail to represent the observed shift toward more frequent high-intensity events from winter to summer. These biases reflect the general tendency for too low summer INT by all models (see Figure 5). Noteworthy model-specific features are the overestimate of low-intensity events for ARPEGE and HIRHAM, ranging up until a threshold of 5 mm, and the steep gradient of the distribution functions for CHRM, HadRM and REMO in the range 1–10 mm/d, suggesting too many low-intensity events among all wet days.

[44] The distributions for spring and autumn (Figures 13b and 13d) show characteristics intermediate to the winter and

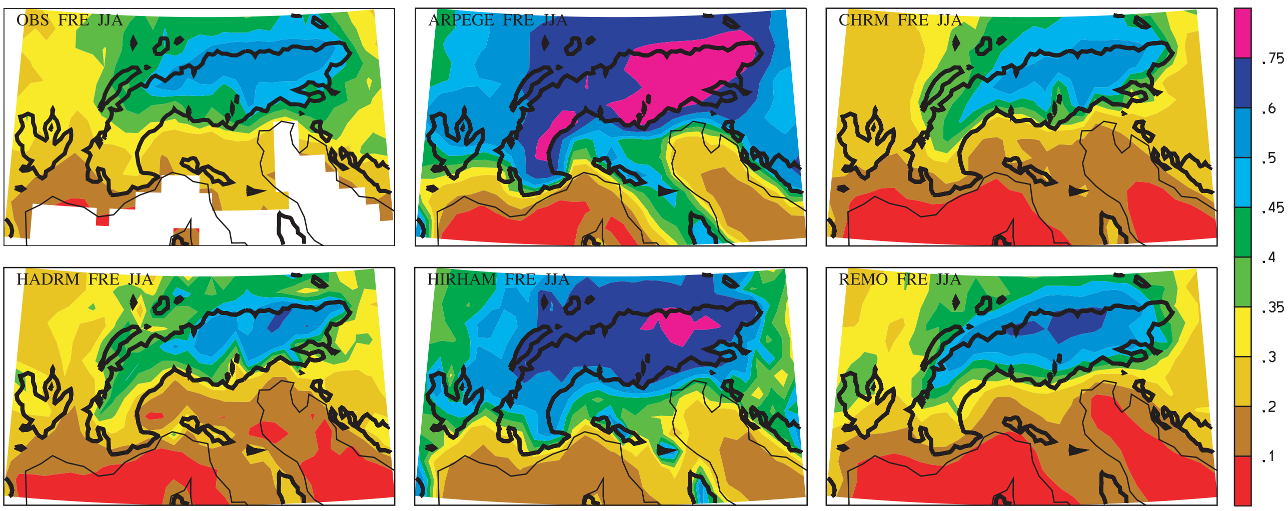

Figure 10. Mean summer (JJA) precipitation frequency (FRE, fraction) for OBS (top left) and models.

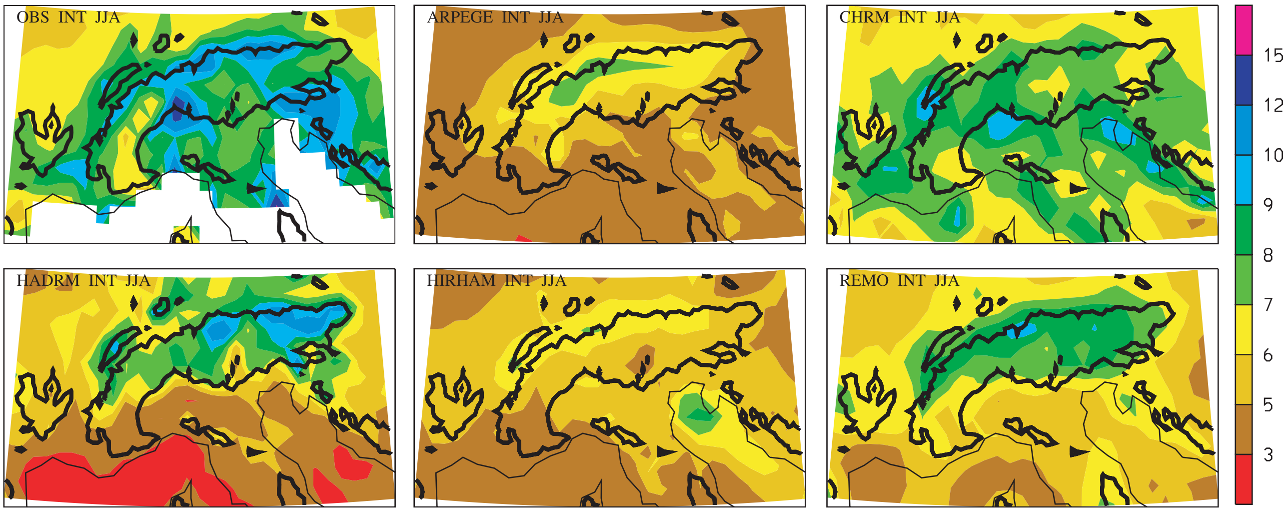

Figure 11. Mean summer (JJA) precipitation intensity (INT, mm/d) for OBS (top left) and models.

summer conditions with a tendency of the models to better represent the upper tail of the observed distribution in spring (similar to winter) and more substantial biases in autumn (similar to but lower in magnitude than in summer).

[45] The distribution functions just discussed are influenced by and carry the signal of model biases in the wet-day frequency and precipitation intensity. To examine the role of these biases, "debiased" frequency distributions were calculated by adjusting each model distribution function to correspond with the observed wet-day frequency and precipitation intensity. The adjustment was undertaken by scaling the conditional wet-day quantiles Qxx with the ratio of seasonal precipitation intensity between OBS and the models. The debiased distributions (Figures 13e–13h) are much closer to the observations than the original distributions. This implies that the major deficiencies in the model distributions are primarily due to FRE and INT biases, rather than errors in the shape of the distributions. Nevertheless some of the model-specific errors remain even after debiasing: HIRHAM in summer and ARPEGE in all seasons (except autumn) exhibit too short tails in the distribution, while HadRM, and to some degree also CHRM, simulate too many high-intensity events in winter and autumn.

4.4. Model Intercomparison for Other European Domains

[46] The Alpine region considered in this evaluation covers only about 5% of the computational domains of the RCMs under consideration. No conclusions can therefore be drawn from this study on the models' skill and biases over the European continent as a whole. However, it is of interest to assess at least, to what extent the characteristic intermodel differences found in the Alpine region are specific to the Alps or prevail in other European regions.

[47] An intercomparison of several daily precipitation statistics from the five models is displayed in Figure 14 for the Alps and four additional European subdomains. (Subdomains are displayed in Figure 1b; only land grid points were taken in the intercomparison.) Observations from the

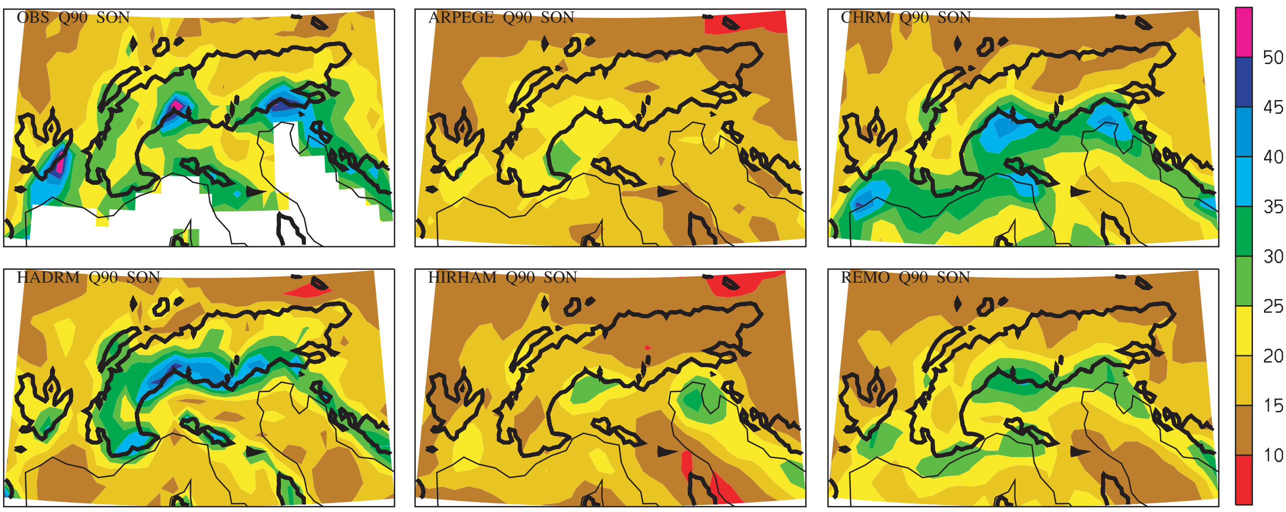

Figure 12. The 90th quantile (Q90) of daily precipitation (mm/d) in autumn (SON) for OBS (top left) and models.

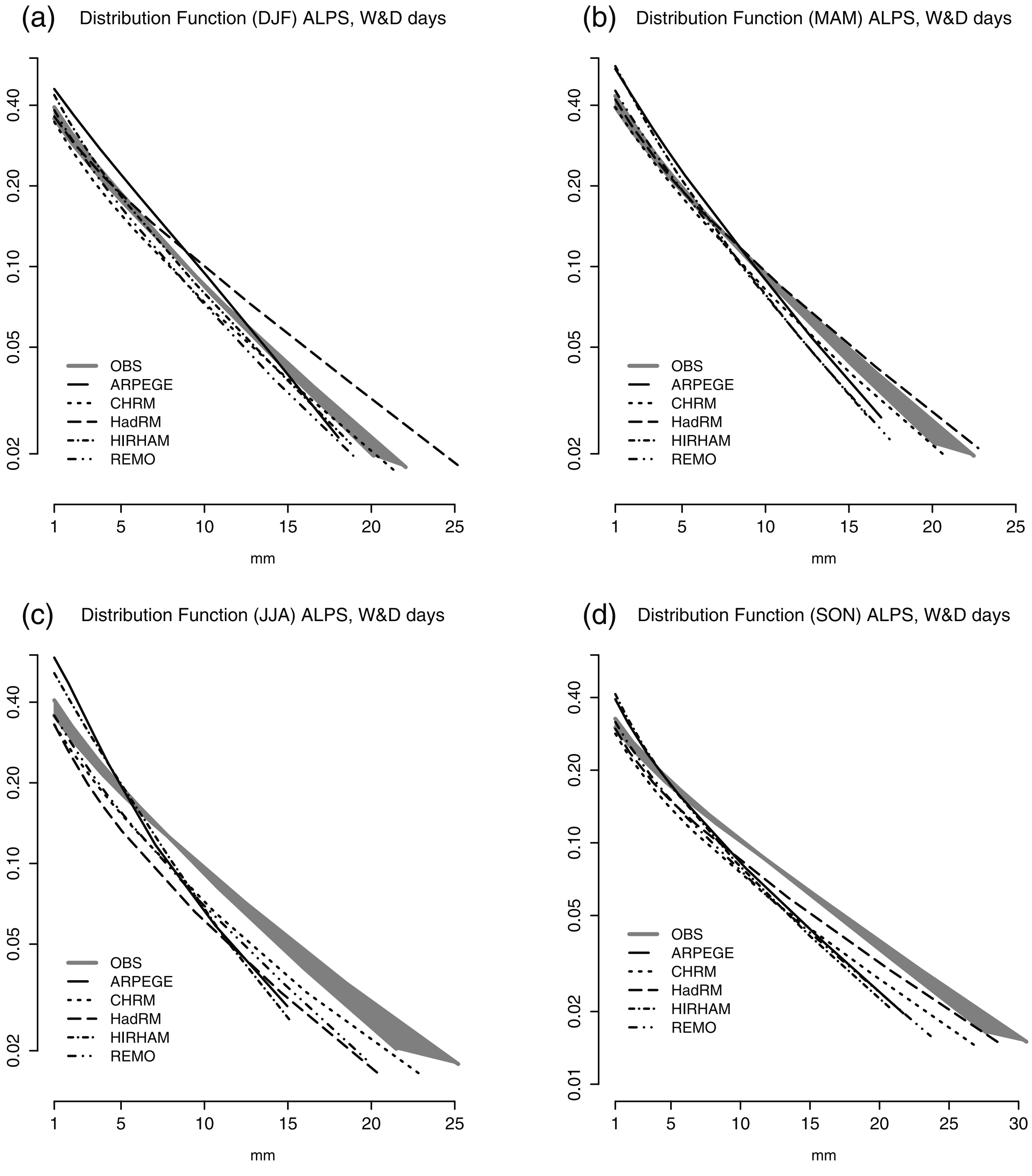

Figure 13. Domain mean frequency distribution of daily grid point precipitation for the Alpine region (AL, Figure 1) in four seasons. Results are shown for the distribution including wet and dry days (panels a–d) and for the debiased distribution (i.e. model distributions are adjusted to FRE and INT of observations, panels e–h). Shaded area for OBS represents results for effective spatial resolutions between 40 and 100 km (scale uncertainty, see section 2.3).

Alpine rain gauge analysis (filled squares) are available exclusively for the Alps. For the remaining regions we make use of the global 0.5° monthly precipitation analysis of the Climatic Research Unit (CRU) [*New et al.*, 1999, 2000] for the same 15-year reference period. CRU results are available for MEA only (full circles in Figure 14).

[48] Mean seasonal precipitation for the Alpine subdomain (AL) differs between the two observational data sets, CRU being 14% smaller in winter and 8% larger in summer compared to the analysis from the high-resolution network (OBS). These discrepancies are due to the smaller station sample available to the CRU analysis. Within the

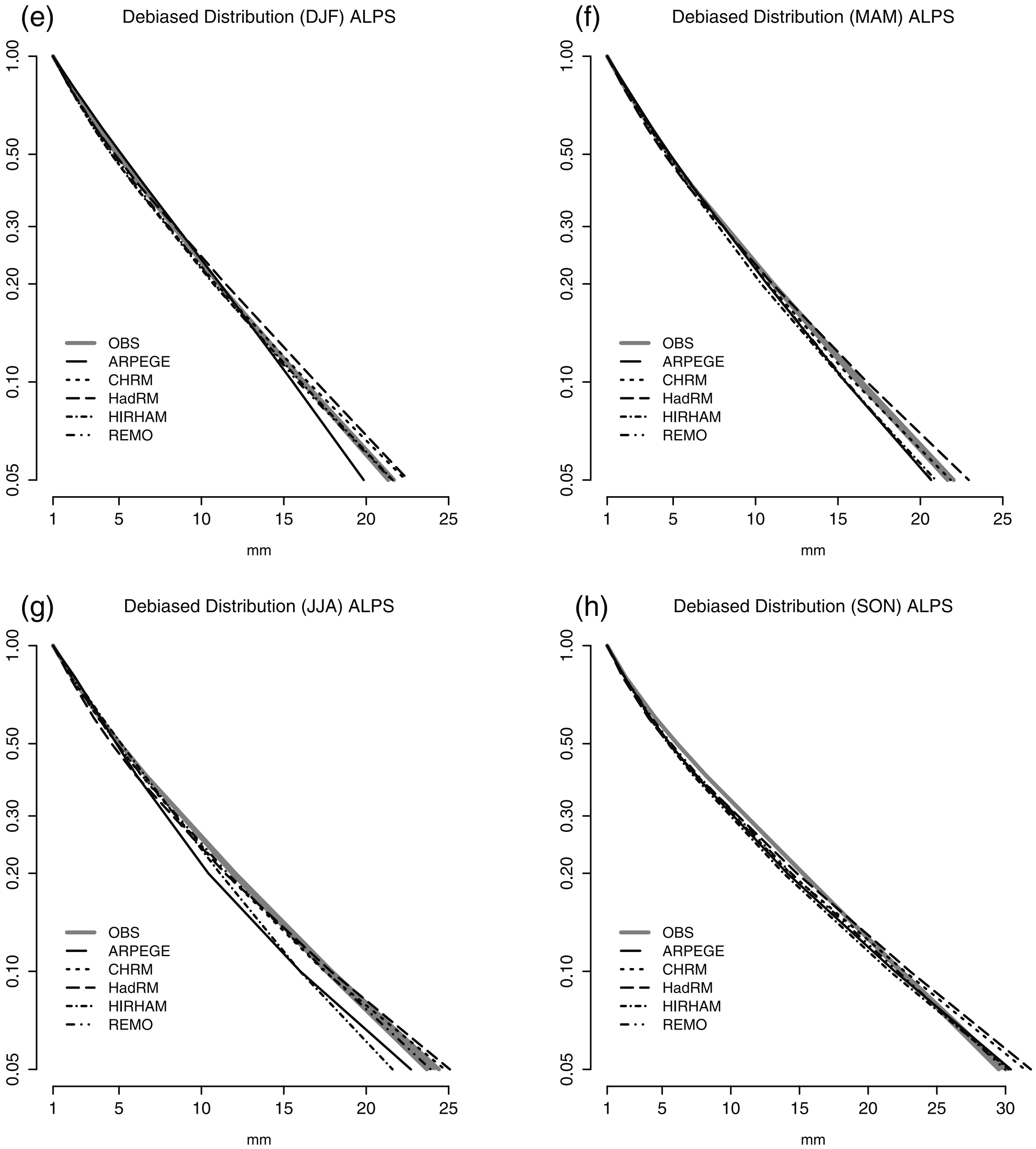

Figure 13. (continued)

Alpine subdomain only about 320 station records were available (M. New, personal communication 2000), and this complicates the demarcation of the various mesoscale features in the CRU analysis. (See also the study of *Frei and Schär* [1998] for a comparison of the two analyses.) This comparison underlines the merit of high-resolution rain gauge data for the present evaluation in the Alps. However, it does not necessarily imply a similar level of observation uncertainty in the other domains. For example a much denser network could be used in the CRU analysis for the British Isles.

[49] The intercomparison (Figure 14) shows that several of the characteristic intermodel differences found for the Alpine region are replicated in the other European regions: ARPEGE and HIRHAM exhibit larger precipitation frequency (FRE) than the other three models in all subdomains. The differences are particularly marked in summer (JJA) but are also present in winter (DJF), except for Scandinavia (SC). On the other hand, CHRM is the model with the lowest FRE, the highest INT and highest Q90 in all subdomains in summer. Note also that REMO has a similar tendency for these parameters. Again, as for the Alps,

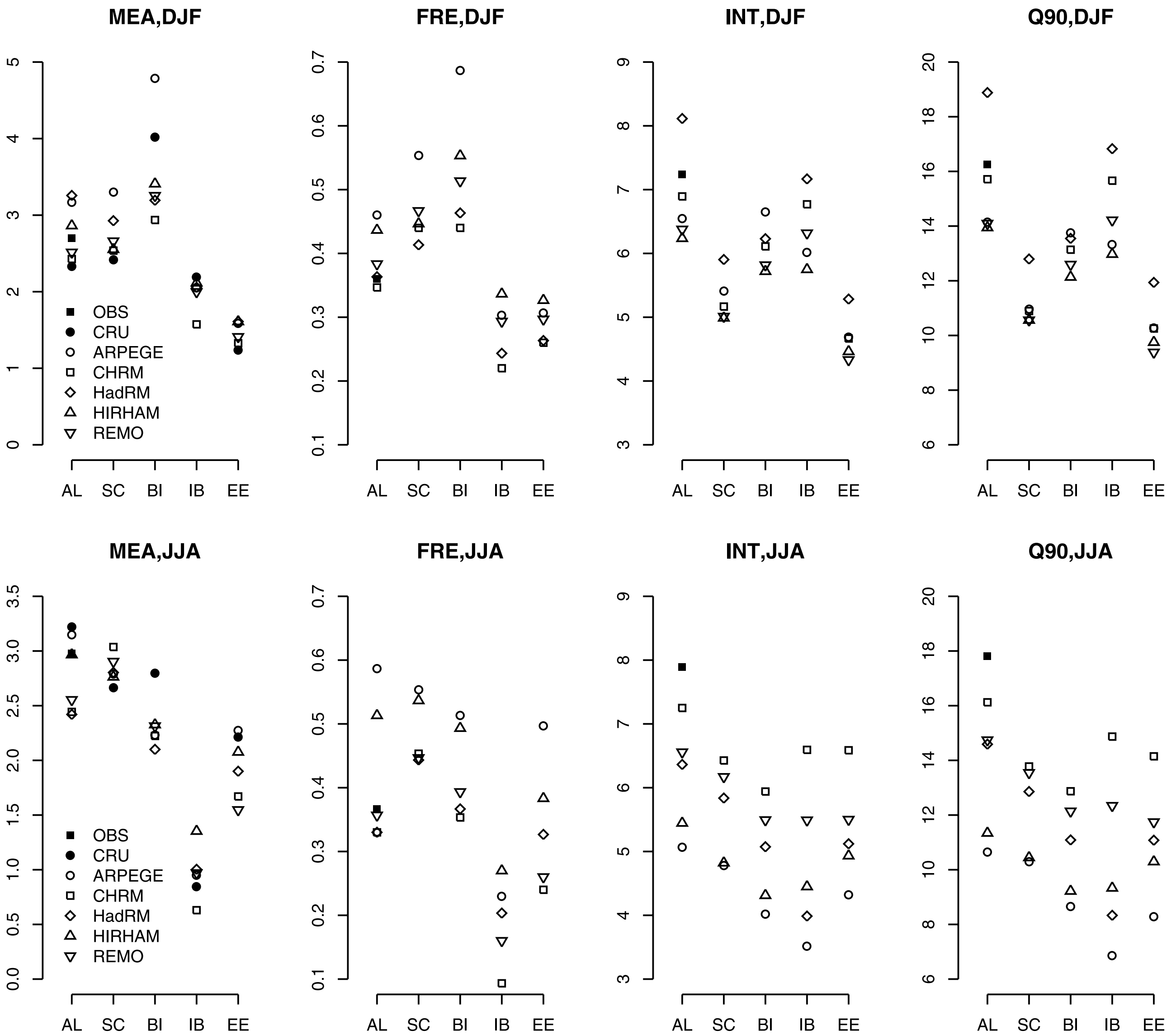

Figure 14. Intercomparison of daily precipitation statistics (domain mean values of MEA, FRE, INT, and Q90, see Table 1) for European regions. Domains (see Figure 1b) are AL, Alps; BI, British Isles; EE, Eastern Europe; IB, Iberian Peninsula; and SC, Scandinavia. A legend of model symbols is given in the top left panel. Observations (filled symbols) are from the Alpine analyses (OBS) and from the Climatic Research Unit global precipitation analysis (CRU) [*New et al.*, 1999, 2000].

HadRM shows higher INT and larger Q90 in winter, than all the other models (except for the British Isles (BI)).

[50] The similarities of this intercomparison with the results for the Alpine region suggest that the major intermodel differences in the precipitation frequency distributions, especially those in summer, are primarily model intrinsic, rather than region dependent. While the long-tailed distributions seem to be more consistent with observations in the Alpine region, this is not necessarily the case for the other regions. An evaluation against detailed observations across several regions would be required to answer this question.

5. Conclusions

[51] A detailed evaluation has been undertaken of the daily precipitation statistics as simulated by 4 limited area climate models and 1 variable-resolution global climate model. The evaluation was carried out by reference to a daily observational analysis which, due to the exceptional density of the underlying rain gauge network, has allowed for an evaluation on scales near the models' grid resolution of 50 km.

[52] The evaluation did not identify a single best model. Each model shows reasonable performance for some statistics but substantial deviations for others. The performance for individual statistics varies considerably between the models and this intermodel variability tends to be larger for the daily statistics (wet-day frequency, intensity and high quantiles) than for mean seasonal precipitation.

[53] For mean precipitation the models reproduce the main characteristics of the annual cycle and the seasonal variation in the subridge-scale distribution. However, three models (CHRM, HadRM, and REMO) underestimate summer mean

conditions by 25%. Depending on the model, this bias is related to three factors of the daily precipitation statistics: too weak precipitation intensity, a too short-tailed frequency distribution and/or a too low wet-day frequency. The two models with less deficient summer mean conditions (ARPEGE and HIRHAM) exhibit even stronger underestimates of summer precipitation intensity, but this is (almost) compensated by an overestimate in wet-day frequency. In winter, the model biases for the daily statistics are similar in character to those in summer, but they are smaller in magnitude. Comparisons for other European regions suggest that the most prominent intermodel differences found in the Alpine region are not merely region specific but seem to display model-inherent features. However, this does not imply that biases are necessarily similar in nature in other European regions, because the precipitation characteristics vary quite substantially across the continent.

[54] Comparing the results of the present evaluation with earlier versions of the same RCMs [e.g., *Christensen et al.*, 1997; *Noguer et al.*, 1998; *Machenhauer et al.*, 1998], it appears that model biases in seasonal mean precipitation have been reduced with the newer generation models (at least in the Alps). Some of these improvements can be attributed to the fact that the regional climate models in this study were forced from observed boundary conditions (ERA15) rather than from GCM integrations of present-day climate [as in *Machenhauer et al.*, 1998]. The systematic bias in circulation is therefore considerably lower: For example the bias in seasonal mean sea level pressure for HIRHAM dropped from ±3 to ±1 hPa [*Christensen et al.*, 2002]. Again the excessive zonality of circulation seen in the earlier ARPEGE integration [*Machenhauer et al.*, 1998] is smaller (though not eliminated) in the new model version discussed here (see A.-L. Gibelin and M. Déqué, Anthropogenic climate change over the Mediterranean region simulated by a global variable resolution model, submitted to *Climate Dynamics*, 2002). On the other hand there is also clear evidence that some reduction of the precipitation bias is due to the changes implemented to parameterization packages in the models [cf. *Noguer et al.*, 1998; *Christensen et al.*, 2002].

[55] Despite the general improvements, the simulation of too dry conditions over parts of the summer half-year, remains a prominent task for model improvement. In the Alpine region this drying problem is mostly evident for the months of August and September, while the conditions during early summer (June and July) are reasonably simulated (see Figure 5). The summer dryness is a continued problem of climate models in the Mediterranean region and southeastern Europe, found in analysis driven RCMs [e.g., *Noguer et al.*, 1998; *Murphy*, 1999; *Hagemann et al.*, 2001], in GCM driven RCMs [e.g., *Machenhauer et al.*, 1998] and in global high-resolution models [e.g., *Wild et al.*, 1997]. Deficiencies in the parameterizations for convection, the soil physics and land surface parameters, and the surface radiation balance were suggested as possible error sources [*Hagemann et al.*, 2001; *Noguer et al.*, 1998; *Wild et al.*, 1997]. The present evaluation suggests that the cause of summer dryness in the Alps is likely model dependent. The spatial distribution of the bias and its relation to biases in wet-day frequency and precipitation intensity differs considerably between the models considered. Even for those two models with a comparatively good simulation of summer mean precipitation, the summer drying issue remains in terms of the considerable and mutually compensating biases in the daily statistics.

[56] It is noteworthy that the present evaluation does not hint toward specific errors of particular physical parameterizations as regards the simulation of daily precipitation statistics. In fact, the two models sharing similar parameterization packages (HIRHAM and REMO) differ considerably in their representation of the statistics, while the two models with similar error structure in all statistics (CHRM and REMO), share the same dynamical core, but differ in parameterization package (see section 3). This intriguing result suggests that the simulation of daily precipitation statistics is sensitive to a variety of model components including the dynamics, physical parameterization, and their interplay.

[57] A promising result of this evaluation is that the RCMs have shown to reproduce the most prominent patterns of the spatial distribution of seasonal precipitation in the Alps. Most of the models exhibit a climatology of heavy precipitation (as represented by the 90% quantile) which is in reasonable agreement with the observed spatial distribution at the scale of the major mesoscale (i.e., 200 km) variations of the Alpine ridge (though not necessarily at the scale of the model grid spacing). Note that these distributions are complex and do not merely depict elevation dependence. The agreement provides confidence that RCMs are capable of simulating the major mesoscale precipitation processes responsible for the subridge-scale variations in the precipitation climate, and it attests the models capability as climate downscaling tools.

[58] The evaluation of the present study has focused on the time-mean error structure (i.e., systematic errors). An interesting extension would be the consideration of time dependence in the model errors (i.e., random errors). Such an extension would allow quantifying the model performance with respect to the year-by-year variations in the various statistics and would provide insights of the model performance in relation to climate anomalies. Focussing on mean seasonal precipitation over Europe, analyses along these lines are described for one of the models (CHRM) by Vidale et al. (submitted manuscript, 2002) and for earlier versions of the other models by *Christensen et al.* [1997] and *Murphy* [1999]. A systematic analysis and intercomparison in the Alpine region embracing some of the daily statistics will be the subject of a subsequent study.

[59] **Acknowledgments.** This research was supported by the Fifth Framework Program of the European Union (project MERCURE, contract ENV4-CT97-0485), by the Swiss Ministry for Education and Science (BBW contract 97.008), and by the UK Department for Environment, Food and Rural Affairs (DEFRA) Climate Prediction Programme (PECD 7/12/37). Additional support was provided by the Swiss National Science Foundation (NCCR Climate). We are indebted to the following institutes for providing access to daily precipitation data: DWD, Offenbach, Germany; Hydrogr. Zentralbüro, Vienna, Austria; ZAMG, Vienna, Austria; Météo France, Toulouse, France; UCEA, Rome, Italy; MeteoSwiss, Zürich, Switzerland; SIMN, Rome, Italy; Meteorological Service, Zagreb, Croatia; and Hydrometeorological Institute, Ljubljana, Slovenia. The gridded surface climatology used in section 4.4 has been supplied by the Climate Impacts LINK Project (Department of the Environment contract PECD7:12:96) on behalf of the Climatic Research Unit in Norwich, UK.

References

Beljaars, A. C. M., and P. Viterbo, The role of the boundary layer in a Numerical Weather Prediction model, in *Clear and Cloudy Boundary*

Layers, edited by A. A. M. Holstlag and P. G. Duynkerke, pp. 287–304, R. Neth. Acad. of Arts and Sci., Netherlands, 1998.

Bougeault, P., A simple parameterization of the large-scale effects of cumulus convection, *Mon. Weather Rev.*, *113*, 2108–2121, 1985.

Buzzi, A., and L. Foschini, Mesoscale meteorological features associated with heavy precipitation in the Southern Alpine region, *Meteorol. Atmos. Phys.*, *72*, 131–146, 2000.

Christensen, O. B., Relaxation of soil variables in a regional climate model, *Tellus*, *51A*, 674–685, 1999.

Christensen, J. H., O. B. Christensen, P. Lopez, E. Van Meijgaard, and M. Botzet, The HIRHAM4 regional atmospheric climate model, *Sci. Rep. 96-4*, 51 pp., DMI, Copenhagen, 1996.

Christensen, J. H., B. Machenhauer, R. G. Jones, C. Schär, P. M. Ruti, M. Castro, and G. Visconti, Validation of present-day climate simulations over Europe: LAM simulations with observed boundary conditions, *Clim. Dyn.*, *13*, 489–506, 1997.

Christensen, O. B., J. H. Christensen, B. Machenhauer, and M. Botzet, Very high-resolution regional climate simulations over Scandinavia: Present climate, *J. Clim.*, *11*, 3204–3229, 1998.

Christensen, J. H., J. Räisänen, T. Iversen, D. Bjorge, O. B. Christensen, and M. Rummukainen, A synthesis of regional climate change simulations: A Scandinavian perspective, *Geophys. Res. Lett.*, *28*, 1003–1006, 2001a.

Christensen, J. H., O. B. Christensen, and J.-P. Schulz, Contribution from the Danish Meteorological Institute to the MERCURE Final Report (December 1997–November 2000), 2001b.

Christensen, J. H., O. B. Christensen, J.-P. Schulz, S. Hagemann, and M. Botzet, High resolution physiographic data set for HIRHAM4: An application to a 50 km horizontal resolution domain covering Europe, *DMI Tech. Rep. 01-15*, 21 pp., 2001c.

Christensen, J. H., O. B. Christensen, and P. Schulz, Contribution to the MERCURE Final Report (Dec 1997–Nov 2000), internal report of the Danish Meterol. Inst., Copenhagen, Denmark, 2002.

Cox, P. M., R. A. Betts, C. B. Bunton, R. L. H. Essery, P. R. Rowntree, and J. Smith, The impact of new land surface physics on the GCM simulation of climate and climate sensitivity, *Clim. Dyn.*, *15*, 183–203, 1999.

Cusack, S., J. M. Edwards, and R. Kershaw, Estimating the subgrid variance of saturation, and its parameterization for use in a GCM cloud scheme, *Q. J. R. Meteorol. Soc.*, *125*, 3057–3076, 1999.

Dai, A., F. Giorgi, and K. E. Trenberth, Observed and model-simulated diurnal cycles of precipitation over the contiguous United States, *J. Geophys. Res.*, *104*, 6377–6402, 1999.

Daly, C., R. P. Neilson, and D. L. Phillips, A statistical-topographic model for mapping climatological precipitation over mountainous terrain, *J. Appl. Meteorol.*, *33*, 140–158, 1994.

Davies, H. C., A lateral boundary formulation for multi-level prediction models, *Q. J. R. Meteorol. Soc.*, *102*, 405–418, 1976.

Déqué, M., and J. P. Piedelievre, High-resolution climate simulations over Europe, *Clim. Dyn.*, *11*, 321–339, 1995.

Déqué, M., P. Marquet, and R. G. Jones, Simulation of climate change over Europe using a global variable resolution general circulation model, *Clim. Dyn.*, *14*, 173–189, 1998.

Dickinson, R. E., Modeling evapotranspiration for three-dimensional global climate models, in *Climate Processes and Climate Sensitivity*, *Geophys. Monogr. Ser.*, vol. 29, edited by J. E. Hansen and T. Takahashi, pp. 58–72, AGU, Washington, D. C., 1984.

Douville, H., S. Planton, J. F. Royer, D. B. Stephenson, S. Tyteca, L. Kergoat, S. Lafont, and R. A. Betts, The importance of vegetation feedbacks in doubled-CO2 time-slice experiments, *J. Geophys. Res.*, *105*, 14,841–14,861, 2000.

Dümenil, L., and E. Todini, A rainfall-runoff scheme for use in the Hamburg climate model, in *Advances in Theoretical Hydrology*, *EGS Ser. Hydrol. Sci.*, vol. 1, edited by J. P. O'Kane, pp. 129–157, Elsevier Sci., New York, 1992.

Durman, C. F., J. M. Gregory, D. C. Hassell, R. G. Jones, and J. M. Murphy, A comparison of extreme European daily precipitation simulated by a global and a regional climate model for present and future climates, *Q. J. R. Meteorol. Soc.*, *127*, 1005–1015, 2001.

Edwards, J. M., and A. Slingo, Studies with a flexible new radiation code, 1, Choosing a configuration for a large-scale model, *Q. J. R. Meteorol. Soc.*, *122*, 689–720, 1996.

Frei, C., and C. Schär, The frequency of heavy Alpine precipitation events: Results from the updated rain-gauge dataset, *MAP Newsl.*, *7*, 50–51, 1997.

Frei, C., and C. Schär, A precipitation climatology of the Alps from high-resolution rain-gauge observations, *Int. J. Climatol.*, *18*, 873–900, 1998.

Frei, C., C. Schär, D. Lüthi, and H. C. Davies, Heavy precipitation processes in a warmer climate, *Geophys. Res. Lett.*, *25*, 1431–1434, 1998.

Gates, W. L., et al., An overview of the results of the Atmospheric Model Intercomparison Project (AMIP I), *Bull. Am. Meteorol. Soc.*, *80*, 29–55, 1999.

Gibson, J. K., P. Kallberg, S. Uppala, A. Hernandey, A. Nomura, and E. Serano, ERA-15 description (version 2), *ECMWF Reanalysis Proj. Rep. Series (Reading UK)*, vol. 1, 74 pp., 1999.

Giorgetta, M., and M. Wild, The water vapour continuum and its representation in ECHAM4, MPI for Meteorol. Rep. 162, 1995.

Giorgi, F., B. Hewitson, J. Christensen, C. Fu, R. Jones, M. Hulme, L. Mearns, H. Von Storch, and P. Whetton, Regional climate information: Evaluation and projections, in *Climate Change 2001: The Scientific Basis, Contribution of Working Group I to the Third Assessment Report of the Intergovernmental Panel on Climate Change*, edited by J. T. Houghton et al., pp. 583–638, Cambridge Univ. Press, New York, 2001.

Goodrich, D. C., M. Faures, D. A. Woolhiser, L. J. Lane, and S. Sorooshian, Measurement and analysis of small-scale convective storm rainfall variability, *J. Hydrol.*, *173*, 283–308, 1995.

Gregory, D., and S. Allen, The effect of convective downdraughts upon NWP and climate simulations, in *Ninth Conference on Numerical Weather Prediction*, pp. 122–123, Am. Meteorol. Soc., Boston, Mass., 1991.

Gregory, D., and P. R. Rowntree, A mass-flux convection scheme with representation of cloud ensemble characteristics and stability dependent closure, *Mon. Weather Rev.*, *118*, 1483–1506, 1990.

Gregory, J. M., Representation of the radiative effect of convective anvils, *Hadley Cent. Tech. Note 9*, Hadley Cent., The Met. Off., Bracknell, 1999.

Gregory, J. M., and J. F. B. Mitchell, Simulation of daily variability of surface temperature and precipitation in the current and 2xCO2 climates of the UKMO climate model, *Q. J. R. Meteorol. Soc.*, *121*, 1451–1476, 1995.

Groisman, P. Y., and D. R. Legates, The accuracy of United States precipitation data, *Bull. Am. Meteorol. Soc.*, *75*, 215–227, 1994.

Hageman, S., M. Botzet, L. Dümenil, and B. Machenhauer, Derivation of global GCM boundary conditions for 1 km land use satellite data, *MPI Rep. 289*, Max-Planck Inst. für Meteorol., Hamburg, 1999.

Hagemann, S., M. Botzet, and B. Machenhauer, The summer drying problem over south-eastern Europe: Sensitivity of the limited area model HIRHAM4 to improvements in physical parameterization and resolution, *Phys. Chem. Earth, Part B*, *26*, 391–396, 2001.

Hagemann, S., B. Machenhauer, O. B. Christensen, M. Déqué, D. Jacob, R. Jones, and P. L. Vidale, Intercomparison of water and energy budgets simulated by regional climate models applied over Europe, *Rep. 338*, Max-Planck Inst. for Meteorol., Hamburg, Germany, 2002.

Hansen, J., et al., Forcings and chaos in interannual to decadal climate change, *J. Geophys. Res.*, *102*, 25,679–25,720, 1997.

Heck, P., D. Lüthi, H. Wernli, and C. Schär, Climate impacts of European-scale anthropogenic vegetation changes: A sensitivity study using a regional climate model, *J. Geophys. Res.*, *106*, 7817–7835, 2001.

Jacob, D., A note to the simulation of the annual and inter-annual variability of the water budget over the Baltic Sea drainage basin, *Meteorol. Atmos. Phys.*, *77*, 61–73, 2001.

Jacob, D., and R. Podzun, Sensitivity studies with the regional climate model REMO, *Meteorol. Atmos. Phys.*, *63*, 119–129, 1997.

Jacob, D., et al., A comprehensive model intercomparison study investigating the water budget during the BALTEX-PIDCAP period, *Meteorol. Atmos. Phys.*, *77*, 19–43, 2001.

Jacobsen, I., and E. Heise, A new economic method for the computation of the surface temperature in numerical models, *Beitr. Phys. Atmos.*, *55*, 128–141, 1982.

Jones, P. D., and P. A. Reid, Assessing future changes in extreme precipitation over Britain using regional climate model integrations, *Int. J. Climatol.*, *21*, 1337–1356, 2001.

Jones, R. G., J. M. Murphy, and M. Noguer, Simulation of climate change over Europe using a nested regional-climate model, 1, Assessment of control climate, including sensitivity to location of lateral boundaries, *Q. J. R. Meteorol. Soc.*, *121*, 1413–1449, 1995.

Jones, R. G., J. M. Murphy, M. Noguer, and A. B. Keen, Simulation of climate change over Europe using a nested regional-climate model, 2, Comparison of driving and regional model responses to a doubling of carbon dioxide, *Q. J. R. Meteorol. Soc.*, *123*, 265–292, 1997.

Källén, E., *HIRLAM Documentation Manual, System 2.5*, Swed. Meteorol. and Hydrol. Inst. (SMHI), S-60176 Norrköping, Sweden), 1996.

Kessler, E., On the distribution and continuity of water substance in atmospheric circulation models, *Meteorol. Monogr.*, *10*, 18–54, 1969.

Kite, G. W., Simulating Columbia River flows with data from regional-scale climate models, *Water Resour. Res.*, *33*, 1275–1285, 1997.

Lau, K.-M., Y. Sud, and J. H. Kim, Intercomparison of hydrologic processes in AMIP GCMs, *Bull. Am. Meteorol. Soc.*, *77*, 2209–2228, 1997.

Lin, Y.-L., R. D. Farley, and H. D. Orville, Bulk parameterization of the snow field in a cloud model, *J. Clim. Appl. Meteorol.*, *22*, 1065–1095, 1983.

Lüthi, D., A. Cress, C. Frei, and C. Schär, Interannual variability and regional climate simulations, *Theor. Appl. Climatol.*, *53*, 185–209, 1996.
Machenhauer, B., The HIRLAM Final Report, *HIRLAM Tech. Rep. 5*, 116 pp., Dan. Meteorol. Inst., Copenhagen, 1988.
Machenhauer, B., M. Windelband, M. Botzet, J. Hesselbjerg, M. Déqué, G. R. Jones, P. M. Ruti, and G. Visconti, Validation and analysis of regional present-day climate and climate change simulations over Europe, *Rep. 275*, 87 pp., Max-Planck Inst. of Meteorol., Hamburg, 1998.
Majewski, D., The Europa Modell of the Deutscher Wetterdienst, in *Proceedings of the ECMWF Seminar on Numerical Methods in Atmospheric Models*, vol. 2, pp. 147–191, Eur. Cent. For Medium-Range Weather Forecasts, Reading, U.K., 1991.
Majewski, D., and R. Schrodin, Short description of the Europa-Modell (EM) and Deutschland-Modell (DM) of the DWD, *Q. Bull.* (April), 1994.
Massacand, A. C., H. Wernli, and H. C. Davies, Heavy precipitation on the Alpine southside: An upper-level precursor, *Geophys. Res. Lett.*, *25*, 1435–1438, 1998.
McGregor, J. L., Regional climate modelling, *Meteorol. Atmos. Phys.*, *63*, 105–117, 1997.
Mearns, L. O., F. Giorgi, and C. McDaniel, Analysis of daily variability of precipitation in a nested regional climate model: Comparison with observations and doubled CO2 results, *Global Planet. Change*, *10*, 55–78, 1995.
Mearns, L. O., C. Rosenzweig, and R. Goldberg, Mean and variance change in climate scenarios: Methods, agricultural applications, and measures of uncertainty, *Clim. Change*, *35*, 367–396, 1997.
Morcrette, J.-J., Description of the radiation scheme in the ECMWF model, ECMWF Tech. Memo. 165, ECMWF, Shinfield Park, Reading, UK, 1989.
Morcrette, J.-J., Impact of changes to the radiation transfer parameterizations plus cloud optical properties in the ECMWF model, *Mon. Weather Rev.*, *118*, 847–873, 1990.
Morcrette, J.-J., Radiation and cloud radiative properties in the ECMWF forecasting system, *J. Geophys. Res.*, *96*, 9121–9132, 1991.
Murphy, J. M., An evaluation of statistical and dynamical techniques for downscaling local climate, *J. Clim.*, *12*, 2256–2284, 1999.
Neff, E. L., How much rain does a rain gage gage?, *J. Hydrol.*, *35*, 213–220, 1977.
Nespor, V., and B. Sevruk, Estimation of wind-induced error of rainfall gauge measurements using a numerical simulation, *J. Atmos. Oceanic. Technol.*, *16*, 450–464, 1999.
New, M., M. Hulme, and P. Jones, Representing twentieth-century space-time climate variability, part 1, Development of a 1961–1990 mean monthly terrestrial climatology, *J. Clim.*, *12*, 829–856, 1999.
New, M., M. Hulme, and P. Jones, Representing twentieth-century space-time climate variability, part 2, Development of 1961–1990 monthly grids of terrestrial surface climate, *J. Clim.*, *13*, 2217–2238, 2000.
Noguer, M., R. G. Jones, and J. M. Murphy, Sources of systematic errors in the climatology of a regional climate model over Europe, *Clim. Dyn.*, *14*, 691–712, 1998.
Nordeng, T.-E., Extended versions of the conservative parameterization scheme at ECMWF and their impact on the mean and transient activity of the model in the tropics, *ECMWF Tech. Memo. 206*, ECMWF, Shinfield Park, Reading, UK, 1994.
Osborn, T. J., and M. Hulme, Development of a relationship between station and grid-box rainday frequencies for climate model evaluation, *J. Clim.*, *10*, 1885–1908, 1997.
Pan, Z., E. Takle, M. Segal, and R. Arritt, Simulation of potential impacts of man-made land use changes on U.S. summer climate under various synoptic regimes, *J. Geophys. Res.*, *104*, 6515–6528, 1999.
Pan, Z., J. H. Christensen, R. W. Arritt, W. J. Gutowski, E. S. Takle, and F. Otieno, Evaluation of uncertainties in regional climate change simulations, *J. Geophys. Res.*, *106*, 17,735–17,751, 2001.
Pielke, R. A., R. L. Walko, L. T. Steyaert, P. L. Vidale, G. E. Liston, W. A. Lyons, and T. N. Chase, The influence of anthropogenic landscape changes on weather in South Florida, *Mon. Weather Rev.*, *127*, 1663–1673, 1999.
Pope, V. D., M. Gallani, P. R. Rowntree, and R. A. Stratton, The impact of new physical parameterizations in the Hadley Centre climate model: HadAM3, *Clim. Dyn.*, *16*, 123–146, 2000.
Räisänen, J., and R. Joelsson, Changes in average and extreme precipitation in two regional climate model experiments, *Tellus*, *53A*, 547–566, 2001.
Ricard, J. L., and J. F. Royer, A statistical cloud scheme for use in an AGCM, *Ann. Geophys.*, *11*, 1095–1115, 1993.
Richter, D., Ergebnisse methodischer Untersuchungen zur Korrektur des systematischen Messfehlers des Hellmann-Niederschlagsmessers, in *Bericht des Deutschen Wetterdienstes*, vol. 194, 93 pp., Dtsch. Wetterdienst DWD, Offenbach, Germany, 1995.
Ritter, B., and F. Geleyn, A comprehensive radiation scheme for numerical weather prediction models with potential applications in climate simulations, *Mon. Weather Rev.*, *120*, 303–325, 1992.
Roeckner, E., K. Arpe, L. Bengtsson, M. Christoph, M. Claussen, L. Dümenil, M. Esch, M. Giorgetta, U. Schlese, and U. Schulzweida, The atmospheric general circulation model ECHAM-4: Model description and simulation of present-day climate, *Rep. 218*, 90 pp., Max-Planck Inst. für Meteorol. (MPI), Hamburg, 1996.
Schädler, B. and R. Weingartner, Components of the natural water balance 1961–1990, Plate 6.3, Hydrol. Atlas of Switz., Fed. Off. for Water and Geol., Bern, Switzerland, 2002.
Schär, C., T. D. Davies, C. Frei, H. Wanner, M. Widmann, M. Wild, and H. C. Davies, Current Alpine climate, in *A View From the Alps: Regional Perspectives on Climate Change*, edited by P. Cebon, U. Dahinden, H. C. Davies, D. Imboden, and C. C. Jaeger, pp. 21–72, MIT Press, Cambridge, Mass., 1998.
Schär, C., D. Lüthi, U. Beyerle, and E. Heise, The soil-precipitation feedback: A process study with a regional climate model, *J. Clim.*, *12*, 722–741, 1999.
Schwarb, M., C. Daly, C. Frei, and C. Schär, Mean annual and seasonal precipitation in the European Alps 1971–1990, in *Hydrological Atlas of Switzerland*, Plates 2.6. and 2.7, Landeshydrol. und Geol., Bern, 2001.
Seneviratne, S. I., J. S. Pal, E. A. B. Eltahir, and C. Schär, Summer dryness in a warmer climate: A process study with a regional climate model, *Clim. Dyn.*, *20*, doi:10.1007/s00382-002-0258-4, 69–85, 2002.
Sevruk, B., Systematischer Niederschlagsmessfehler in der Schweiz, in *Der Niederschlag in der Schweiz, Beitr. Geol. Schweiz. Hydrol.*, vol. 31, pp. 65–75, Bundesamt für Wasser und Geol., Bern, Switzerland, 1985.
Shepard, D. S., Computer mapping: The SYMAP interpolation algorithm, in *Spatial Statistics and Models*, edited by G. L. Gaile and C. J. Willmott, pp. 133–145, D. Reidel, Norwell, Mass., 1984.
Skelly, W. C., and A. Henderson-Sellers, Grid-box or grid-point: What type of precipitation data do GCMs deliver to climate impact researchers?, *Int. J. Climatol.*, *16*, 1079–1086, 1996.
Smith, R. N. B., A scheme for predicting layer clouds and their water content in a general circulation model, *Q. J. R. Meteorol. Soc.*, *116*, 435–460, 1990.
Stein, J., E. Richard, J. P. Lafore, J. P. Pinty, N. Asencio, and S. Cosma, High-resolution non-hydrostatic simulations of flash-flood episodes with grid-nesting and ice-phase parameterization, *Meteorol. Atmos. Phys.*, *72*, 203–221, 2000.
Stone, M. C., R. H. Hotchkiss, C. M. Hubbard, T. A. Fontaine, and J. G. Mearns, Impacts of climate change on Missouri River Basin water yield, *J. Am. Water Resour. Assoc.*, *37*, 1119–1129, 2001.
Sundqvist, H., A parameterization scheme for non-convective condensation including prediction of cloud water content, *Q. J. R. Meteorol. Soc.*, *104*, 677–690, 1978.
Sundqvist, H., Parameterization of condensation and associated clouds for weather prediction and general circulation simulations, in *Physically Based Modeling and Simulation of Climate and Climate Change*, edited by M. E. Schlesinger, pp. 433–461, D. Reidel, Norwell, Mass., 1988.
Tiedtke, M., A comprehensive mass flux scheme for cumulus parameterization in large-scale models, *Mon. Weather Rev.*, *117*, 1779–1800, 1989.
Warner, T. T., R. A. Peterson, and R. E. Treadon, A tutorial on lateral boundary conditions as a basic and potentially serious limitation to regional numerical weather prediction, *Bull. Am. Meteorol. Soc.*, *78*, 2599–2617, 1997.
Wild, M., A. Ohmura, and U. Cubasch, GCM simulated surface energy fluxes in climate change experiments, *J. Clim.*, *10*, 3093–3110, 1997.
Willmott, C. J., C. M. Rowe, and W. D. Philpot, Small-scale climate maps: A sensitivity analysis of some common assumptions associated with grid-point interpolation and contouring, *Am. Cartogr.*, *12*, 5–16, 1985.

J. H. Christensen, Danish Meteorological Institute, Copenhagen, Denmark.

M. Déqué, Météo France, Centre National de Recherches Météorologiques, Toulouse, France.

C. Frei and P. L. Vidale, Atmospheric and Climate Science, Eidgenossische Technische Hochschule, Winterthurerstrasse 190, CH-8057 Zurich, Switzerland. (christoph.frei@geo.umnw.ethz.ch)

D. Jacob, Max Planck Institute for Meteorology, Hamburg, Germany.

R. G. Jones, Met Office Hadley Centre, Bracknell, UK.